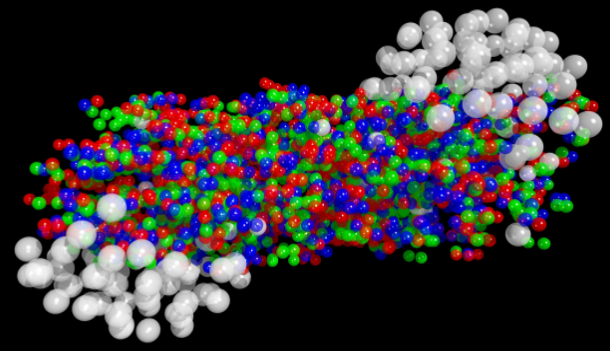
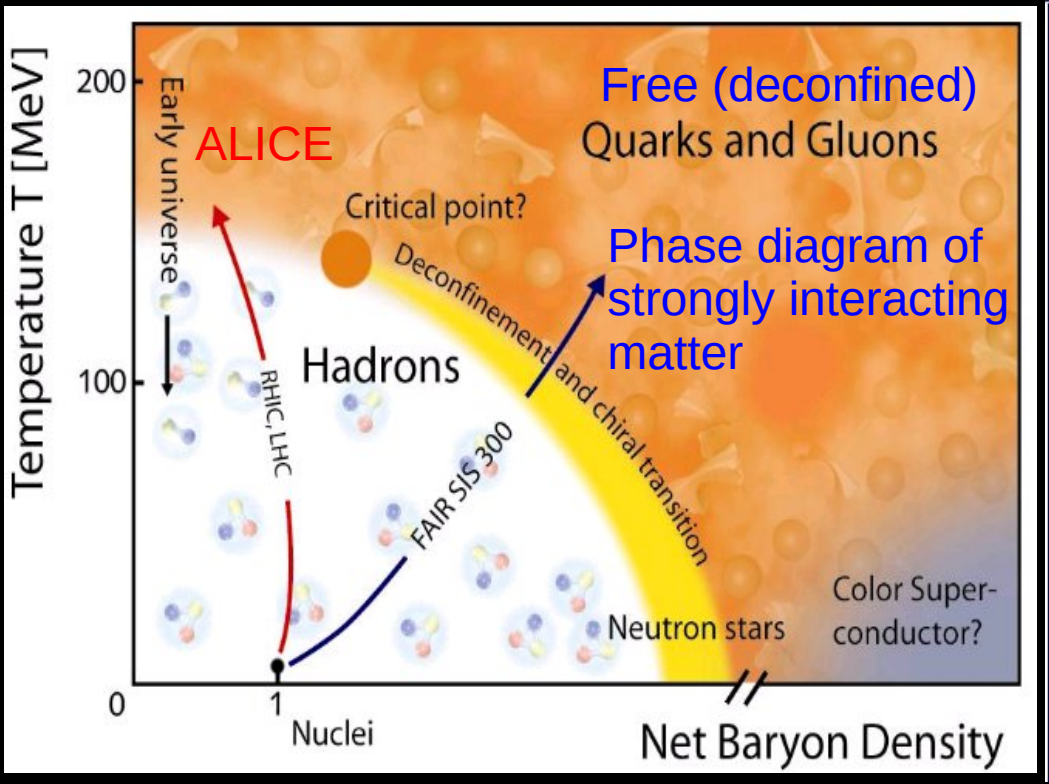
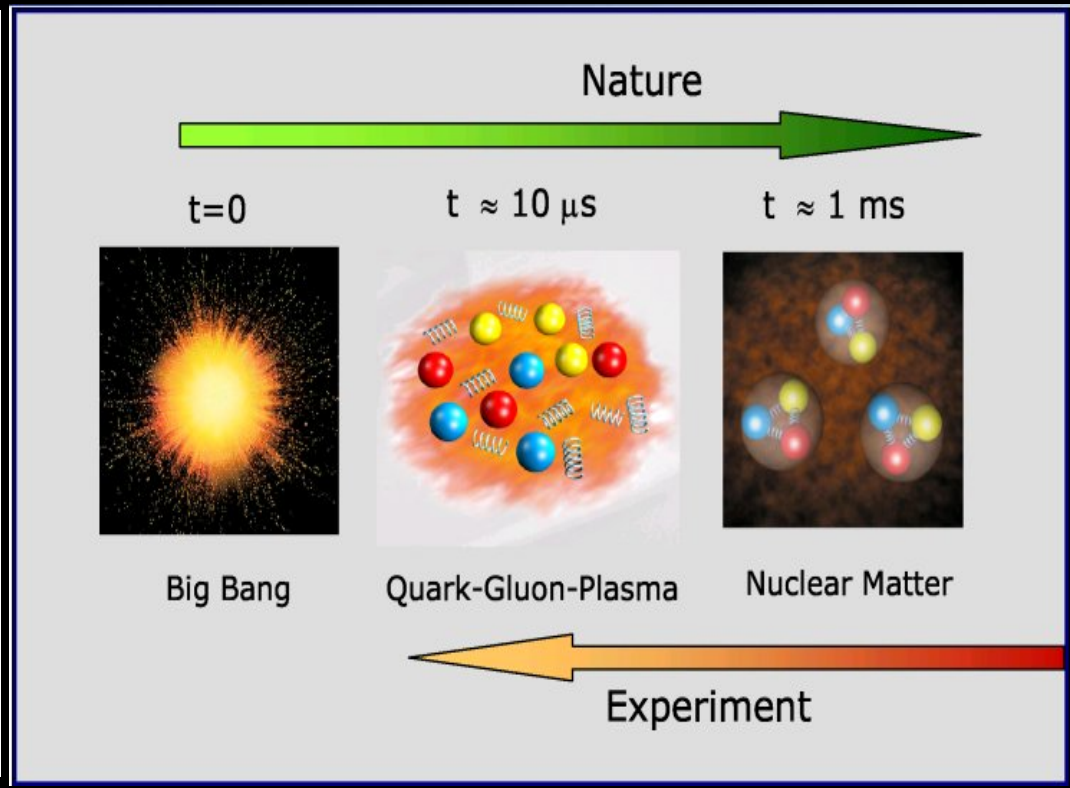
ALICE: Studying QCD matter under extreme conditions

Ultrarelativistic collisions between heavy atomic nuclei: Producing and studying the Quark-Gluon Plasma (QGP), a form of strongly interacting matter created at extreme temperatures and pressures.
Consisting of free quarks and gluons.
A complex many-particle system described by Quantum ChromoDynamics (QCD).
Primordial matter at the birth of the Universe, until ~ 10 μs after the Big Bang, was a QGP.

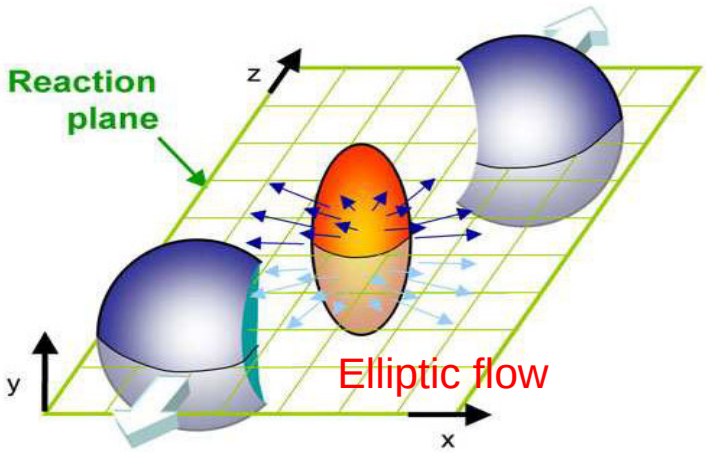


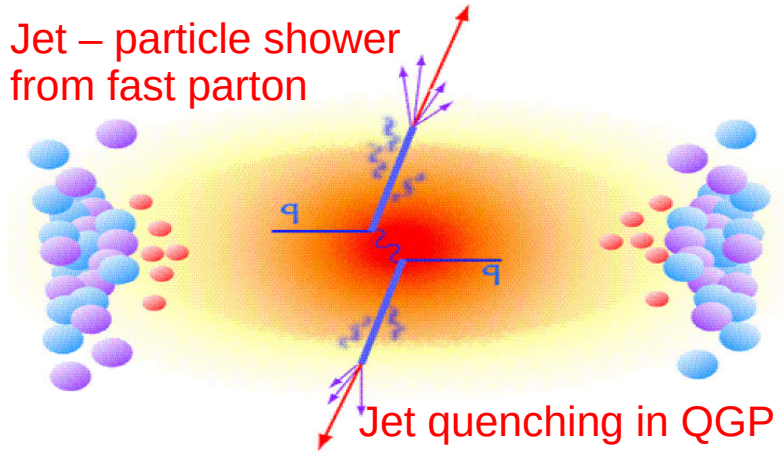




Experimental signatures of the Quark-Gluon Plasma







Studying the QGP properties using known particles as probes. Important to know the system size and geometry.

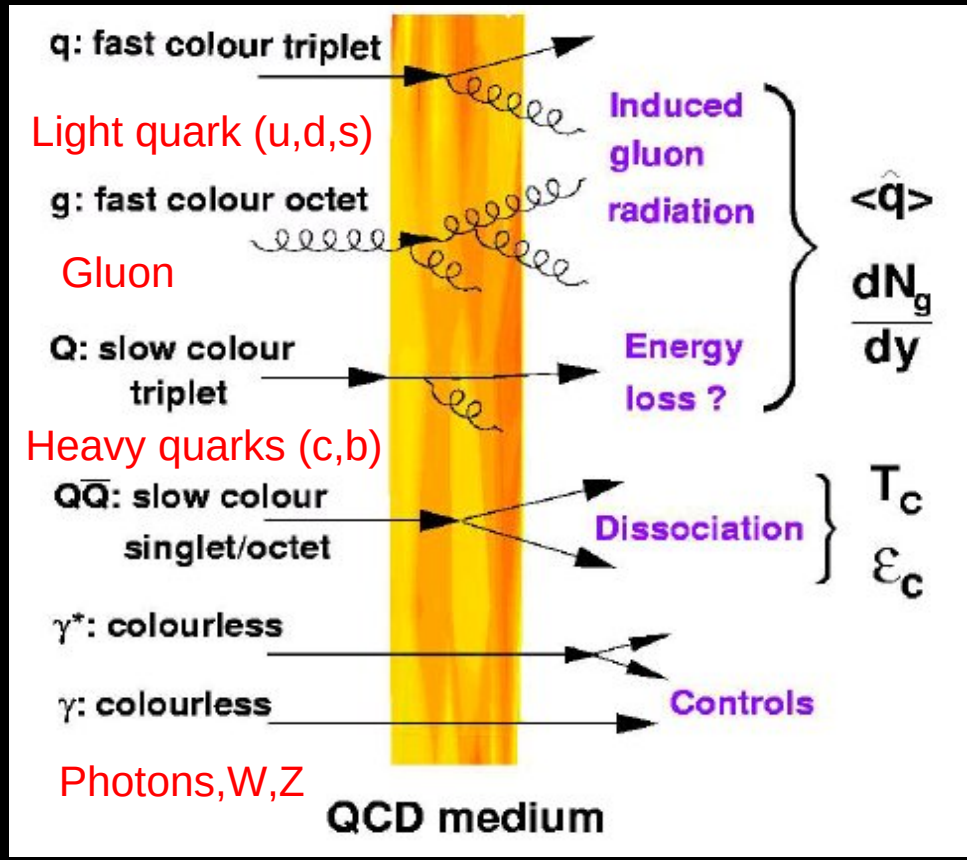
– Collective anisotropic flow: Collision geometry and density fluctuations lead to anisotropic hydrodynamic expansion. QGP is a near-perfect liquid.

– Jet quenching / high-p_T suppression: Coloured partons lose energy traversing a QGP with free colour charges –>

– Medium modifications R_{AA} of specific probes, e.g. jets, high-p_T hadrons, heavy flavour hadrons and quarkonia:

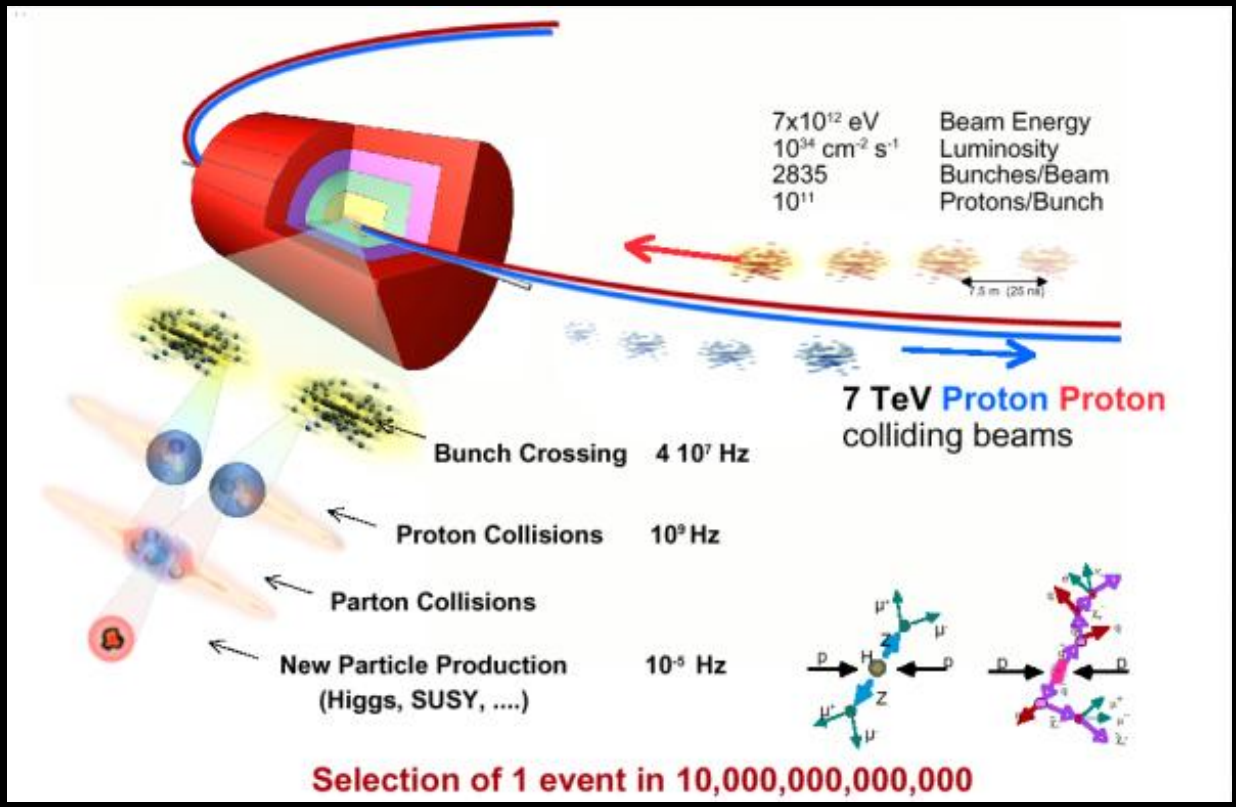
$$R_{AA} = \frac{Y_{AA}}{\langle N_{coll} \rangle Y_{pp}}$$

comparing yields in heavy-ion and pp collisions



Only long-lived particles are directly measured!

Selecting interesting collisions – from pp to Pb-Pb



Production rate *dN/dt* of signals depends on production cross section σ_{prod} and instantaneous luminosity L_{inst} :

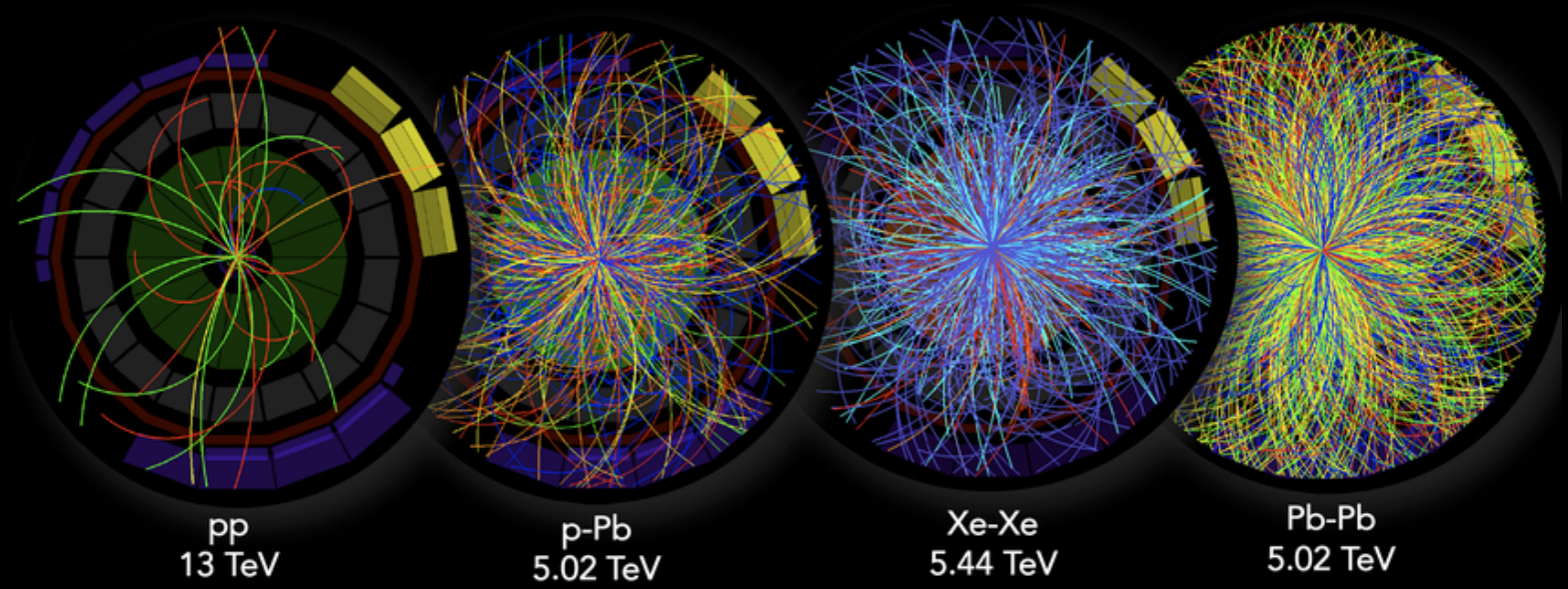
$$\frac{\mathrm{d}N}{\mathrm{d}t} = L_{\mathrm{inst}} \cdot \sigma_{\mathrm{prod}}$$

L_{inst} depends on beam properties; number of particles per beam bunch (N_1, N_2), revolution frequency f, bunch number N_{bunch}, and σ_x,σ_y Gaussian beam widths:

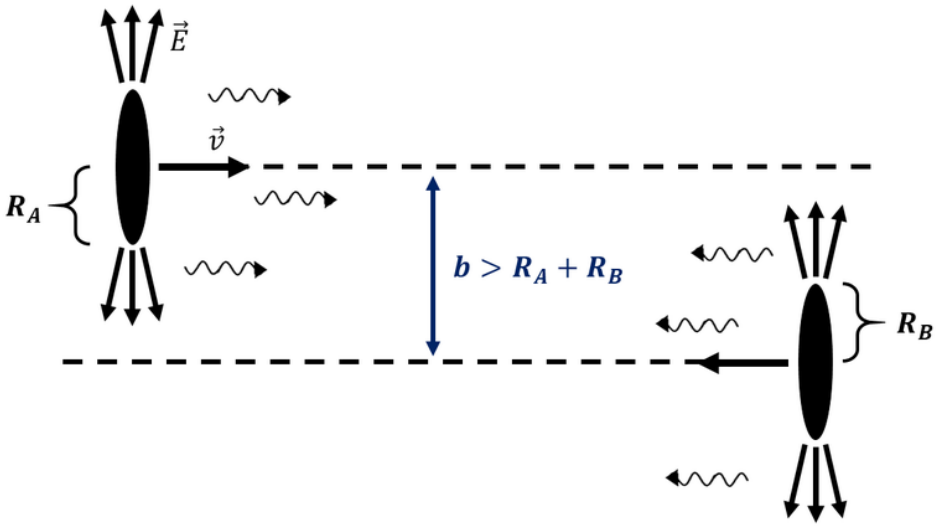
$$L_{\mathrm{inst}} = \frac{N_1 N_2 f N_{\mathrm{bunch}}}{4\pi\sigma_x\sigma_y}$$

High collision rates – need to reject background and select interesting events, using triggers.

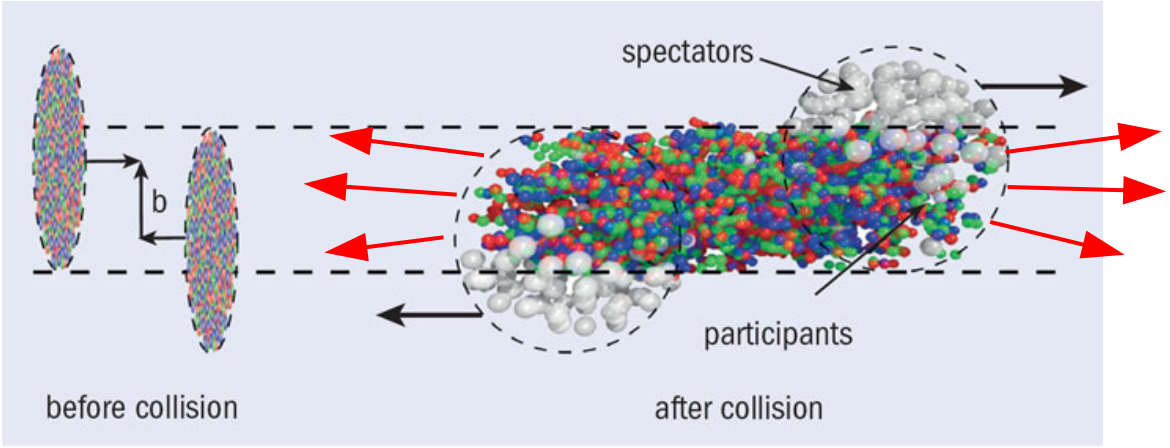
Triggers depend on colliding system (from pp to Pb-Pb). Minimum bias triggers from forward particle production, special triggers on event type or rare signal candidates to study specific phenomena.

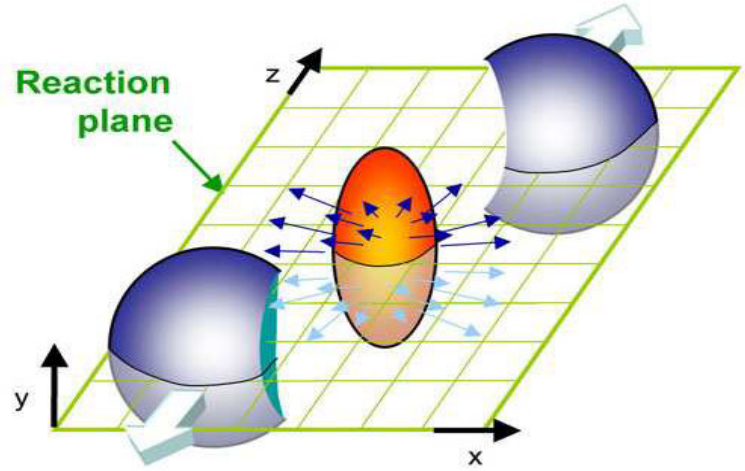


Event properties: Collision geometry



Collision type depends on impact parameter b.
Probability distribution: $P(b)\,db \sim 2\pi\, b\, db$.
Most frequent (largest cross section): Ultraperipheral collisions with $b > R_A + R_B$.
Electromagnetic interactions between collision partners, with copious creation of $e^+ e^-$ pairs and excitation of nuclei followed by nucleon emission.
QGP formation requires collisions with hadronic overlap, $b < R_A + R_B$.



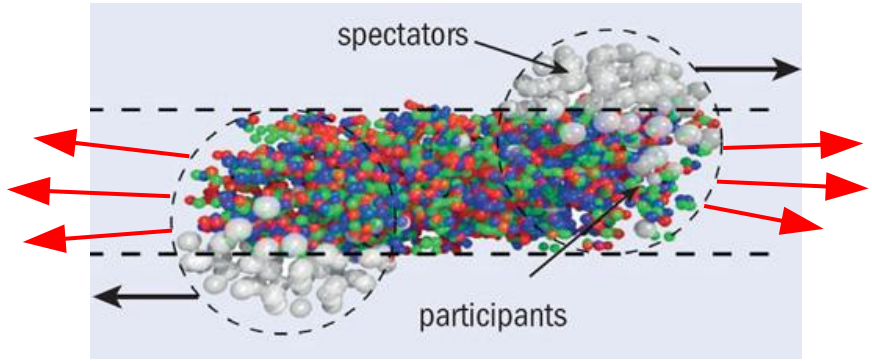


In hadronic collisions:
Non-overlapping parts of nuclei (spectators) continue in beam direction, while overlapping parts (participant zone) form a hot QGP which emits produced particles in all directions, boosted when forward going. Number of produced particles (multiplicity) correlated with size of nuclear overlap region (collision centrality).

Azimuthal distribution of produced particles correlated with orientation of reaction plane, spanned by beam direction and impact parameter vector *b*.
Experimental estimate: Event plane.

The ALICE detector (Run 3 version)

Detectors for triggering and event characterisation



Forward V0 Detector (FV0)

Forward Diffraction Detector (FDD-A)

Zero Degree Calorimeter (ZDC-A)

Beam pipe

Forward Time-0 Detectors (FT0-A and C)

Interaction point (IP)

Zero Degree Calorimeter (ZDC-C)

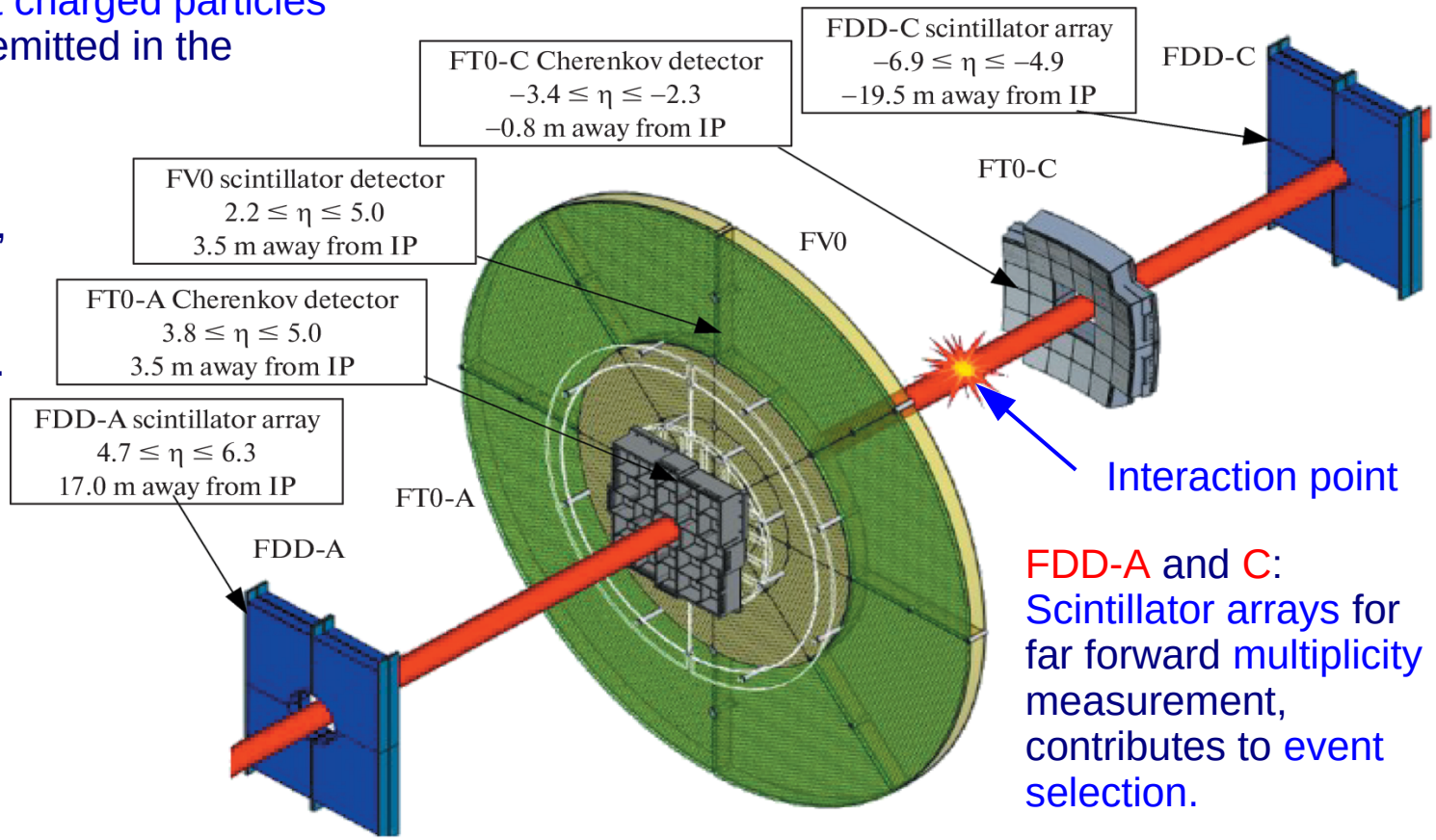
Forward Diffraction Detector (FDD-C)

Fast Interaction Trigger (FIT) detector suite

FIT detectors measure fast charged particles from the participant zone, emitted in the forward direction.

FT0-A and C: Quartz Cherenkov detector arrays, providing precise collision time for time-of-flight measurements (σ ~ 13 ps). Also measures forward charged particle multiplicities for triggering / event selection.

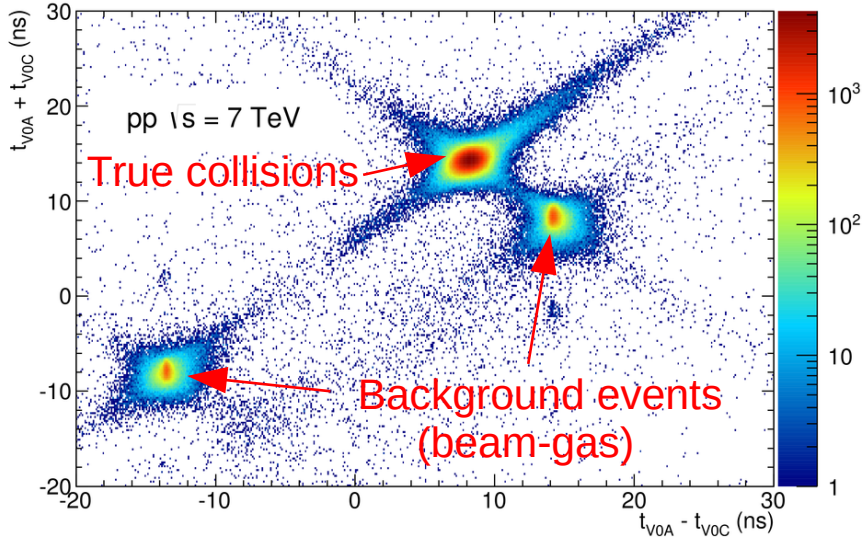
FV0: Large scintillator array for quantitative event characterisation. Provides charged particle multiplicity for centrality determination. Azimuthal segmentation gives good event plane resolution.



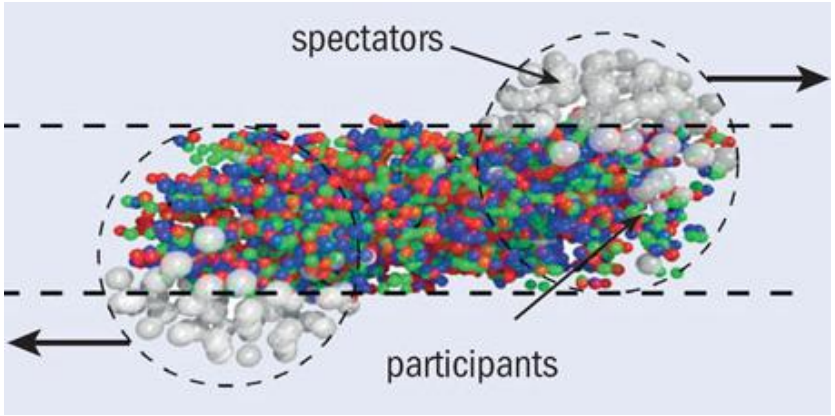
FDD-A and C: Scintillator arrays for far forward multiplicity measurement, contributes to event selection.

Timing must also be correct (correlations between detector arrays and with LHC clock keeping track of beam bunch crossings).

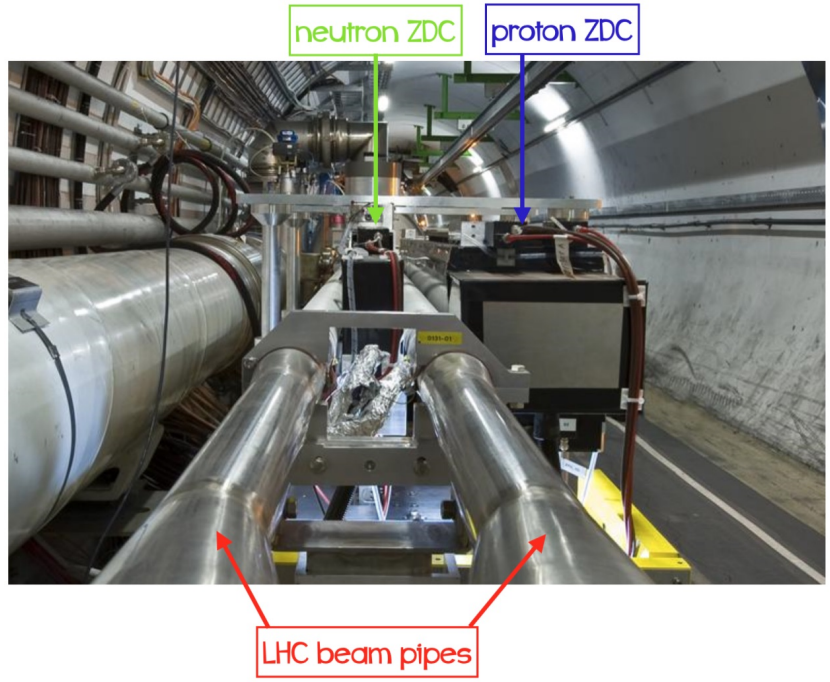
Correlation from sum and difference of signal times in V0A and V0C, on either side of the interaction point (pre-Run 3 setup):



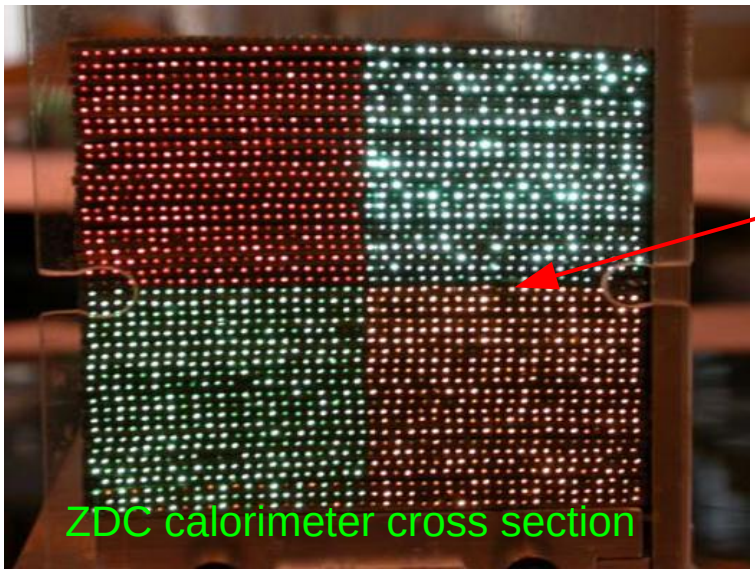
Zero Degree Calorimeters



Spectator regions dissociate and continue in original beam directions while emitting neutrons and protons. Zero Degree Calorimeters stop spectator nucleons in heavy-ion collisions and measure their energy. They also measure nucleons emitted from nuclei excited in electromagnetic interactions.
Neutrons follow straight-line trajectories, protons are deflected by LHC *B*-fields.

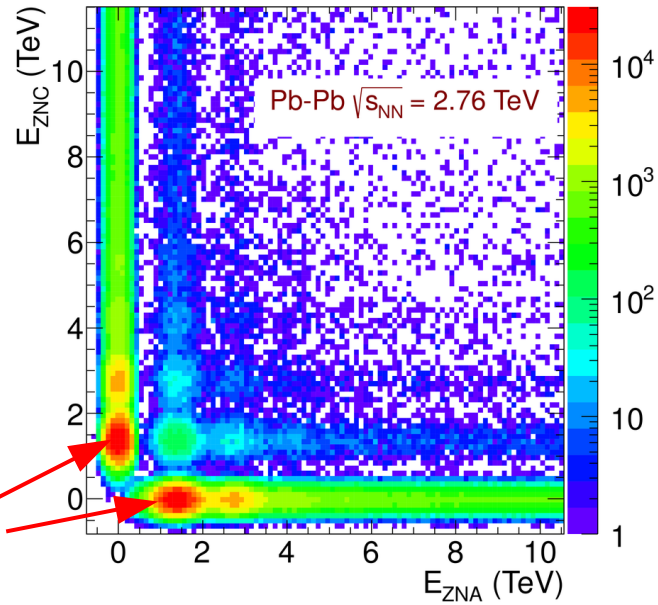


ALICE Zero Degree Calorimeters (A and C): Placed at +– 119 m from IP.



Heavy calorimeter materials: Brass absorber for protons (ZP), tantalum for neutrons (ZN). Quartz optical fibres detect Cherenkov light, ~ proportional to energy deposit.

Correlation between ZN-A and C signals, large signal from EM dissociation events.

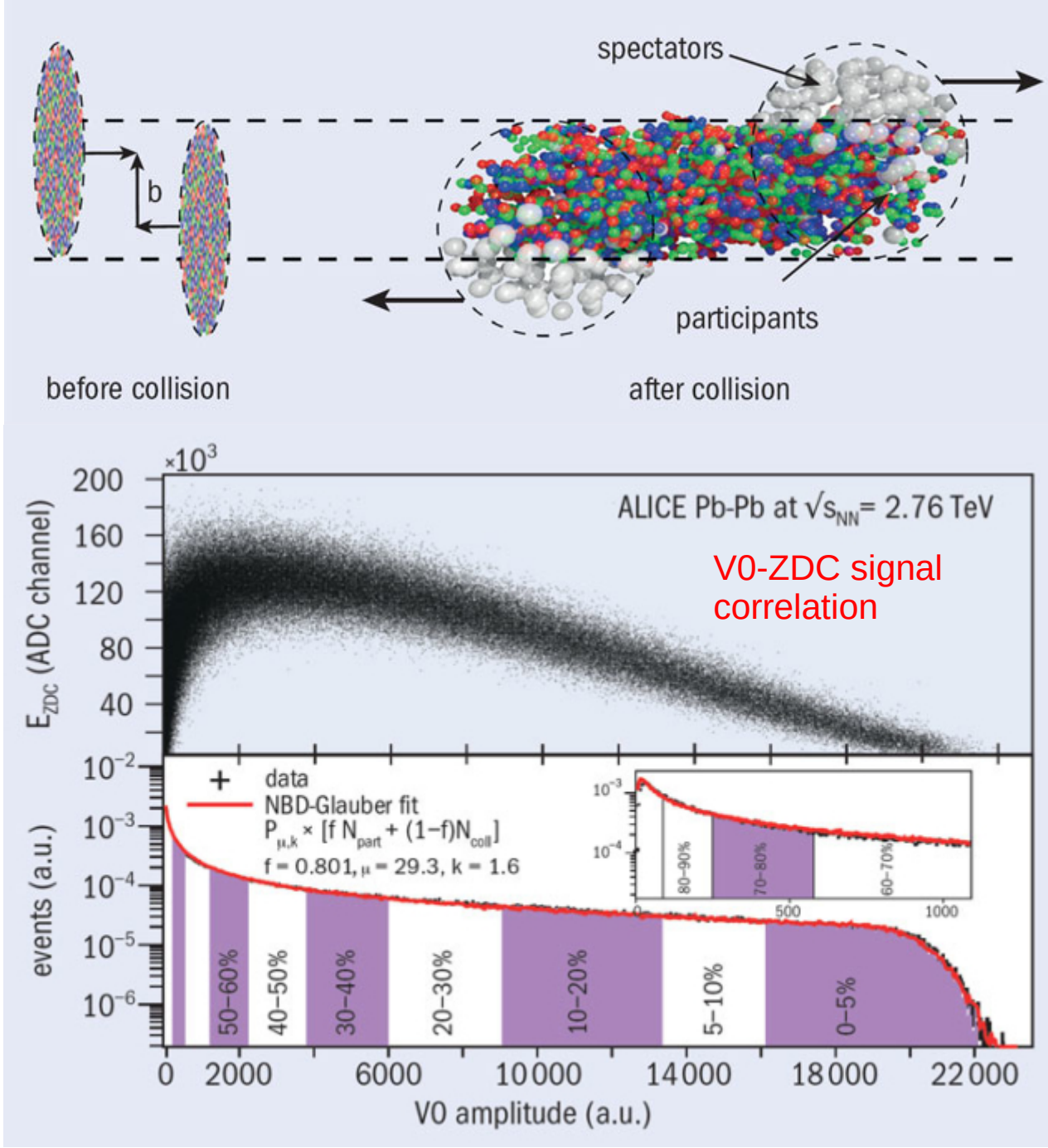


Collision centrality determination with ALICE

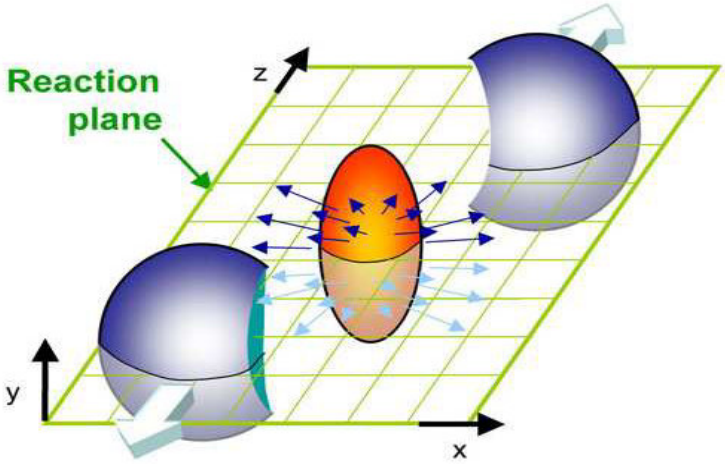
Size of QGP droplet is related to collision centrality, defined by impact parameter *b* (cannot be measured directly). Participants form hot matter, which emits a number of particles (multiplicity) correlated with *b*. Spectators continue with ~ unaltered momenta.

ALICE: Centrality determined fitting the measured multiplicity distribution (in FV0, formerly V0) with a model calculation assuming a geometrical probability distribution for *b*:
$P(b)\,db \sim 2\pi b\,db$;
a realistic nuclear density distribution and a parametrised multiplicity distribution per nucleonic interaction. Centrality classified in percentiles of hadronic cross section, with 0% corresponding to head-on collisions (maximum multiplicity).

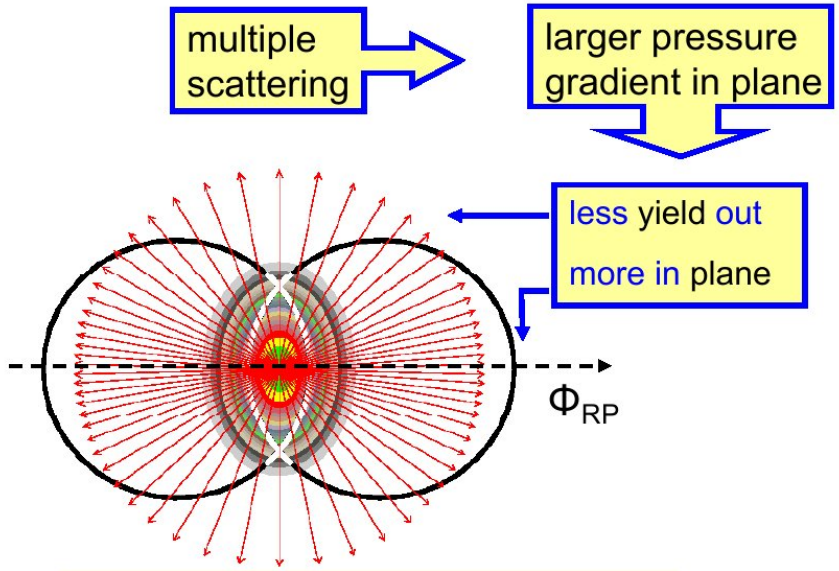
Correlation between V0 multiplicity and ZDC signal: Large ZDC signal for more peripheral collisions (many spectators). Small signal for central and very peripheral collisions, where spectator regions form nuclear fragments caught by neither the ZN nor ZP calorimeters.



Event symmetry plane determination

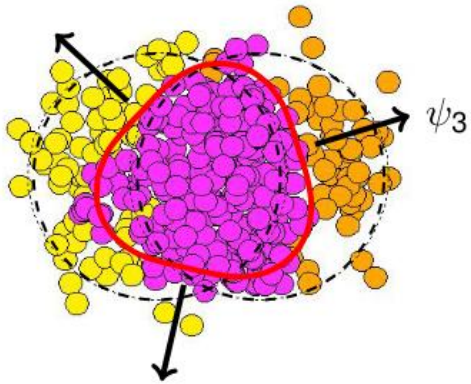


Reaction plane: Defined by beam direction and impact parameter vector *b*.



Non-central collisions gives ~ elliptic participant zone, pressure gradients in the QGP create azimuthally anisotropic particle emission pattern –> measured in the finely segmented FV0 array.

Spectator deflection measured in ZDCs –> estimate of direction of *b* vector.



Density fluctuations in the initial state of the collision partners give higher harmonic anisotropies (*n*).

General decomposition of azimuthal anisotropy using a Fourier series:

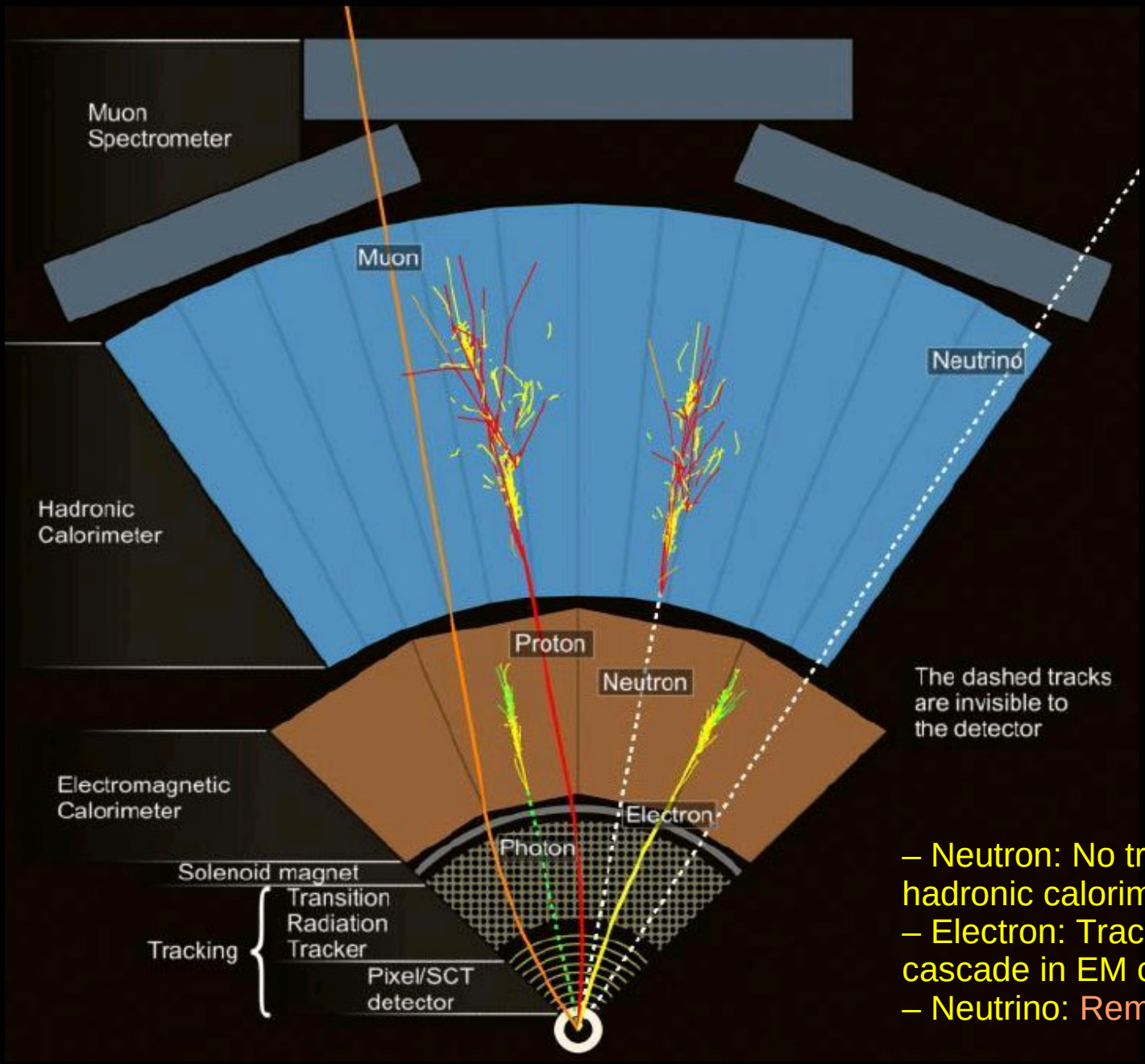
$$\frac{dN}{d\phi} \propto 1 + \Sigma_n v_n \cos\left[n(\phi - \Psi_n)\right] \qquad (n = 1,2,3, \ldots)$$

Event symmetry planes Ψ_n experimentally defined:

$$\Psi_n = \tan^{-1}\left(\frac{Q_{n,y}}{Q_{n,x}}\right) \quad \text{where} \quad Q_{n,x} = \Sigma_j w_j \cos(n\phi_j), \quad Q_{n,y} = \Sigma_j w_j \sin(n\phi_j)$$

Sum over detector segments or tracks. w_j weight factors.

Onion-like detector layout for high-energy physics



From innermost to outermost layer:

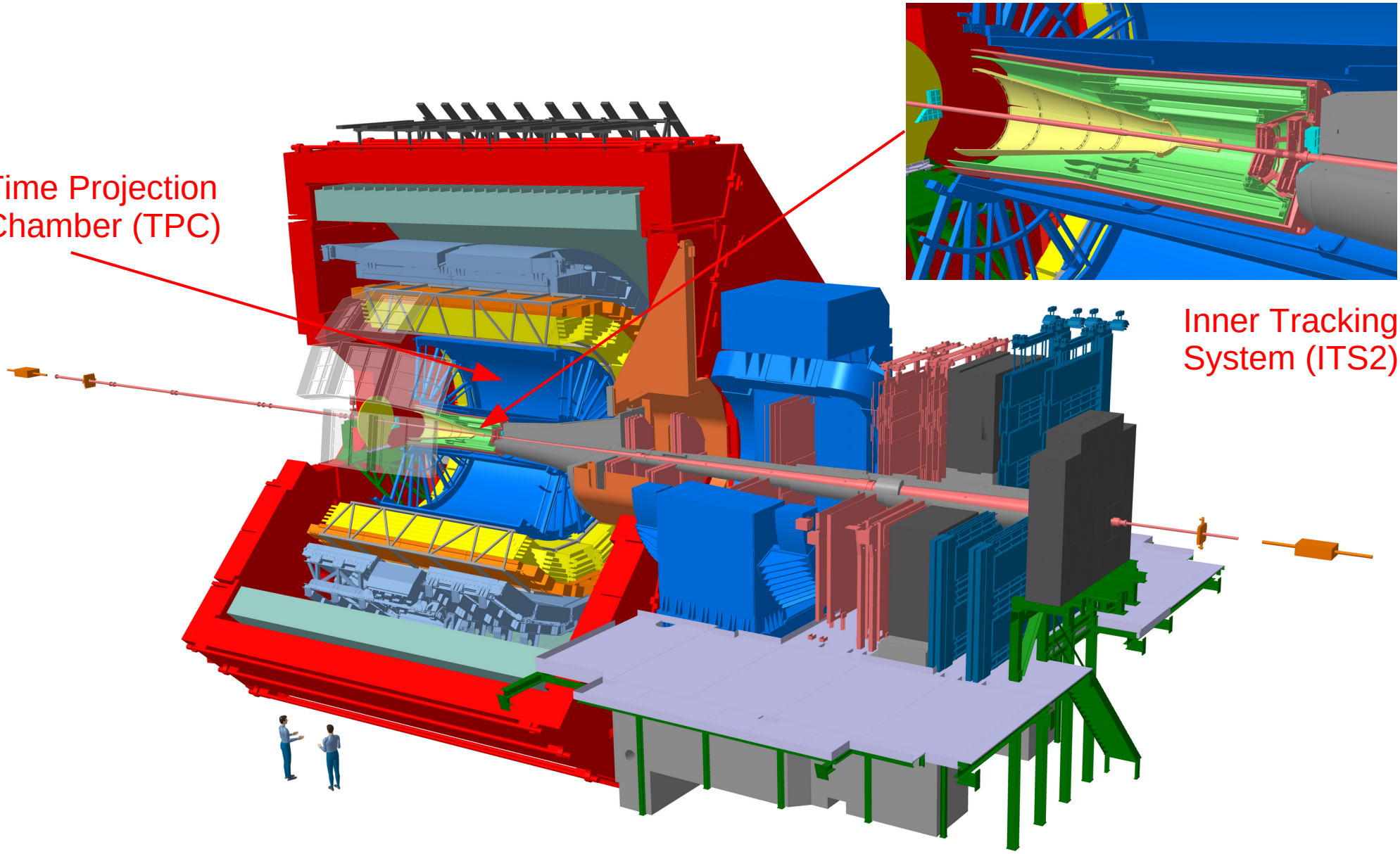
– Vertex detector and other charged particle tracking detectors (with *B* field)
– Electromagnetic calorimeter
– Hadronic calorimeter
– Muon spectrometer

– Muon: Ionisation track in tracking layers, calorimeters, muon spectrometer
– Photon: No track, stops with cascade in EM calorimeter
– Proton: Track in tracking layers and EM calorimeter, stops with cascade in hadronic calorimeter

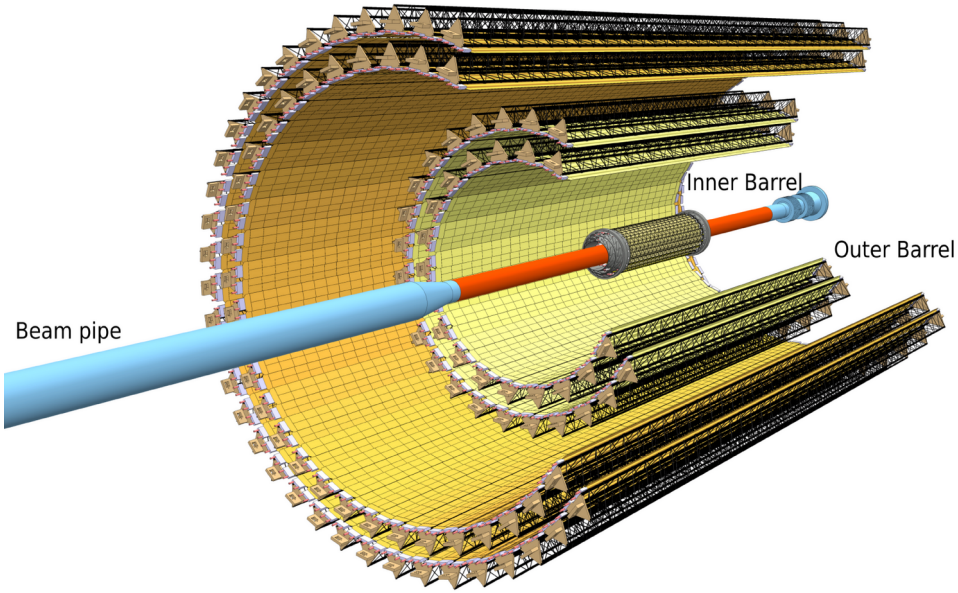
– Neutron: No track, stops with cascade in hadronic calorimeter
– Electron: Track in tracking layers, stops with cascade in EM calorimeter
– Neutrino: Remains invisible in all layers

The ALICE detector (Run 3 version)

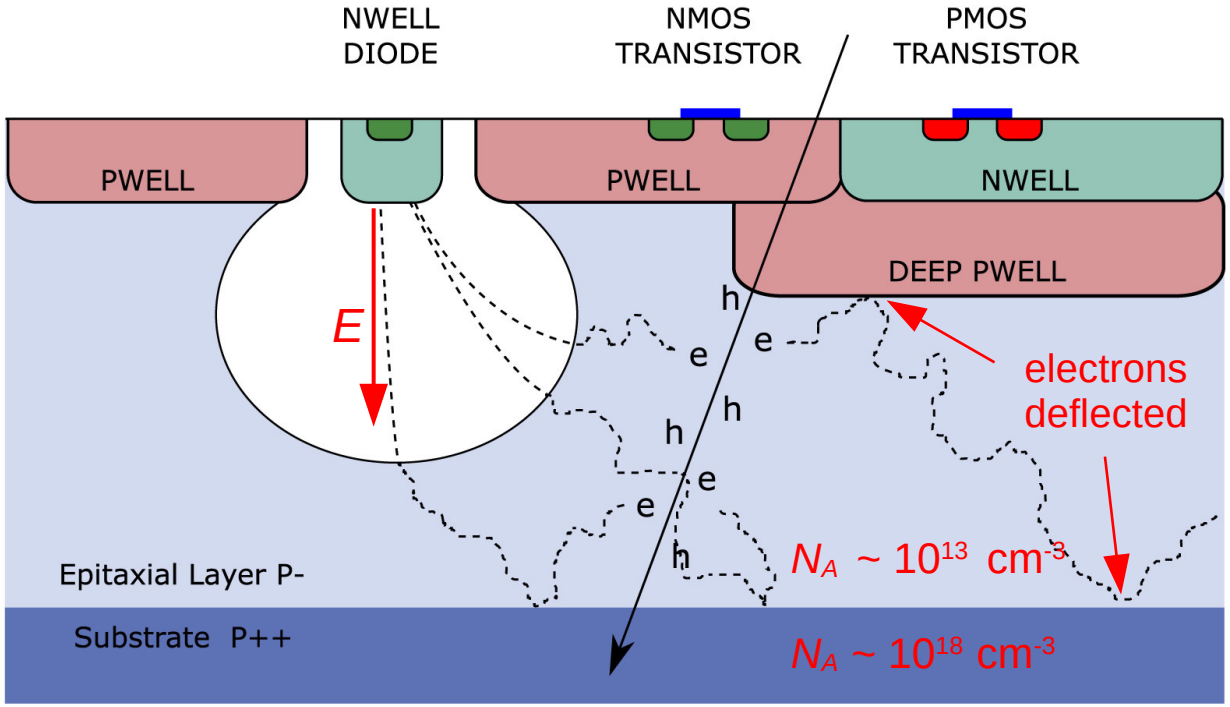
Central barrel main charged particle tracking detectors



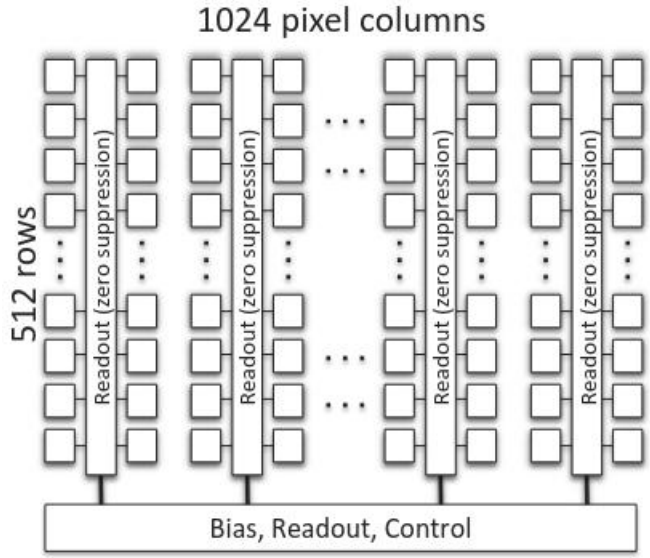
Inner Tracking System (ITS2) – based on Si MAPS



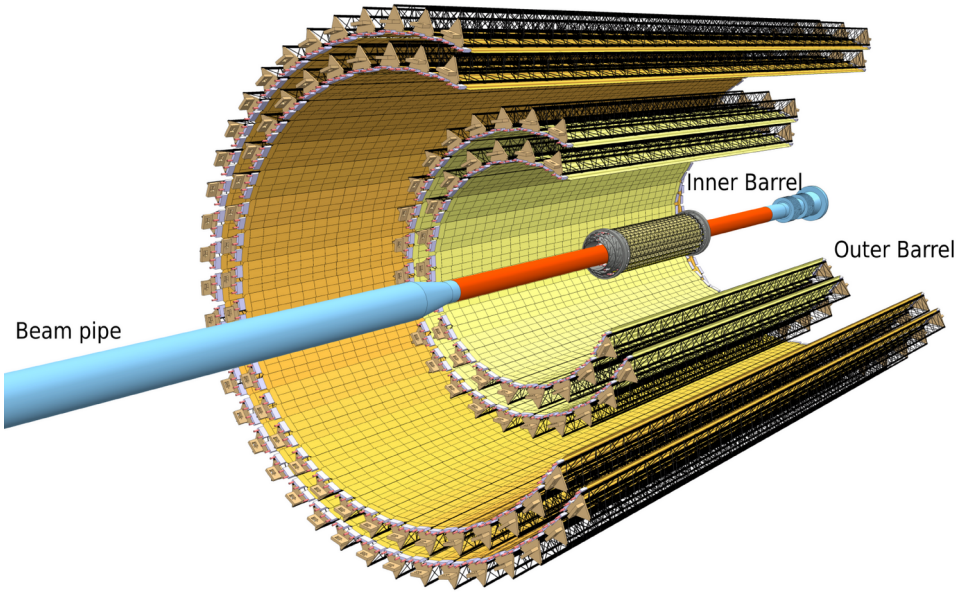
Upgraded ALICE Inner Tracking System (ITS2) for LHC Run 3.
7 Si pixel layers located at R = 2.2 – 39.5 cm.
All layers use Monolithic Active Pixel (MAPS) technology (ALPIDE chip), based on high-resistivity p-type Si as bulk material in wafer (epitaxial layer), electrons collected at nwell diodes (n^+p junctions). High radiation tolerance (important close to interaction point).
Granularity: $r\varphi$ x z = 27 x 29 μm^2.
Resolution: $r\varphi$ x z ~ 5 x 5 μm^2.
ITS1 (Run 1-2): 6 layers, coarser granularity and larger R.)



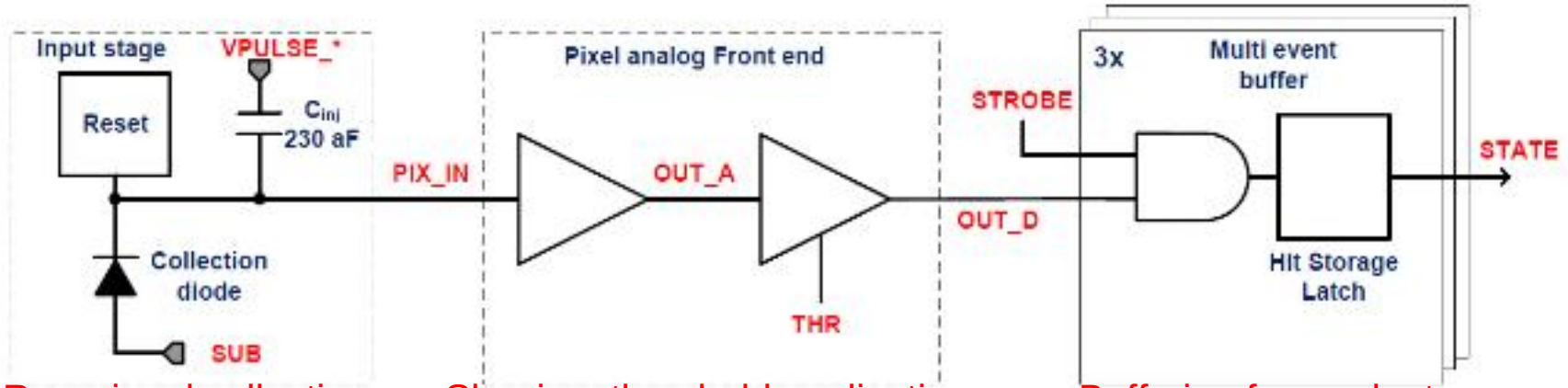
Pixel matrix: 1024 pixel columns with 512 pixels on each side.



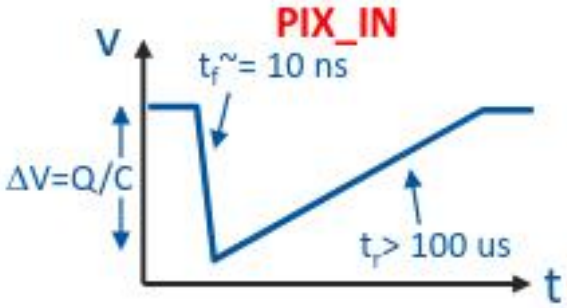
Inner Tracking System (ITS2) signal readout



Binary readout, charge division among neighbouring pixels gives clusters (weight 1/0). Charge collection by diffusion, can work without bias, but reverse bias (~ 3 – 6 V) gives faster charge collection and smaller clusters.
Pixel front-end electronics: Shaping of raw signal, application of adjustable threshold to reject noise –> digital signal, readout on strobe –> data stored in multi-event buffer (up to 3 events). State signal sent to chip peripheral electronics. Supports triggered and continuous readout.



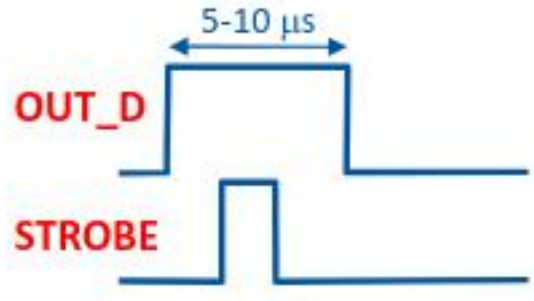
Raw signal collection | Shaping, threshold application | Buffering for readout



Analog

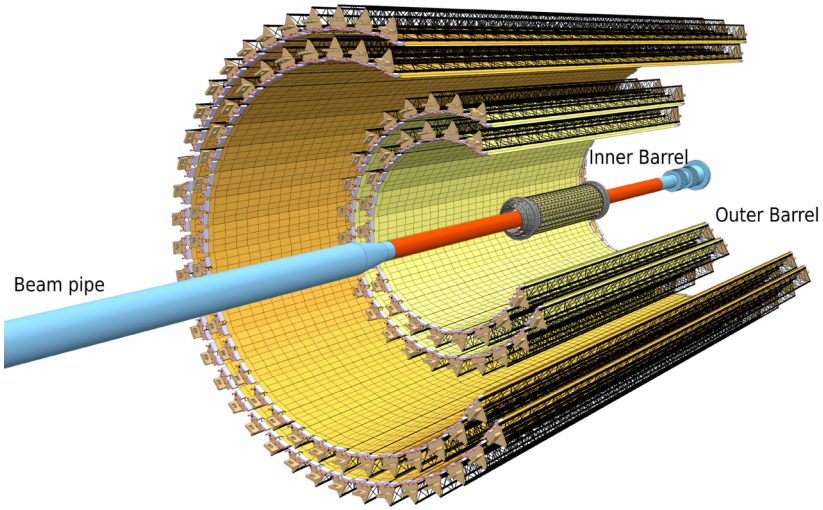


Analog –> digital

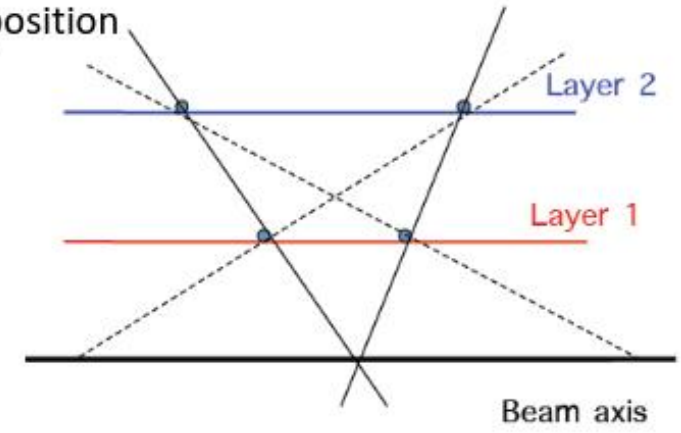


Digital

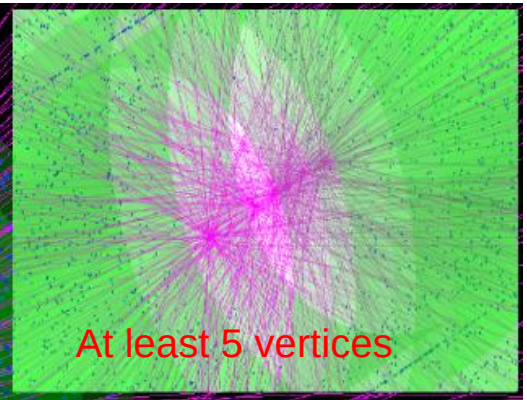
Inner Tracking System (ITS2) primary vertex finding



Primary vertex determination: Tracklets (lines between 2 clusters in different layers) extrapolated back towards beamline, primary vertex where a maximum of tracklets converge.

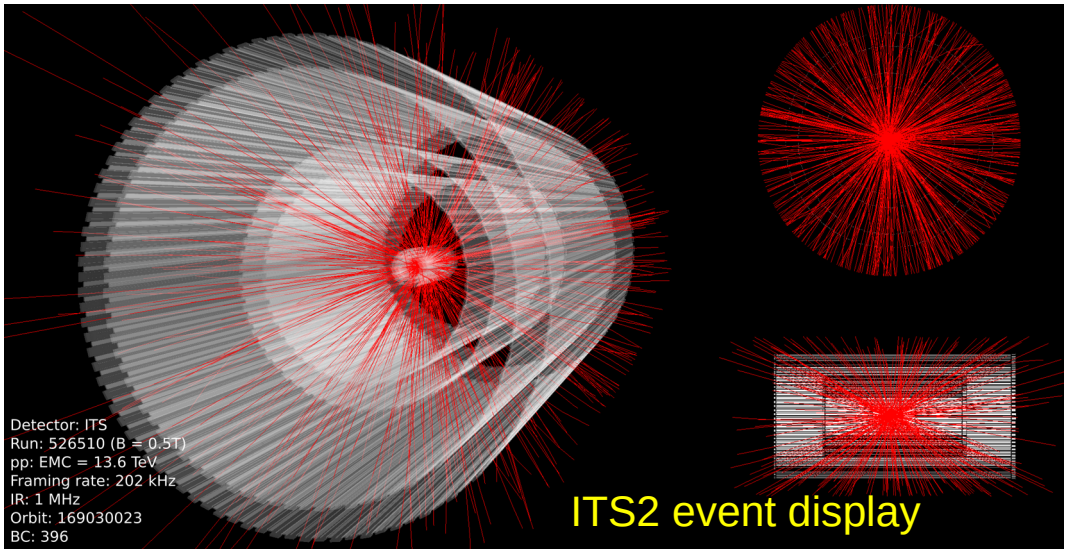


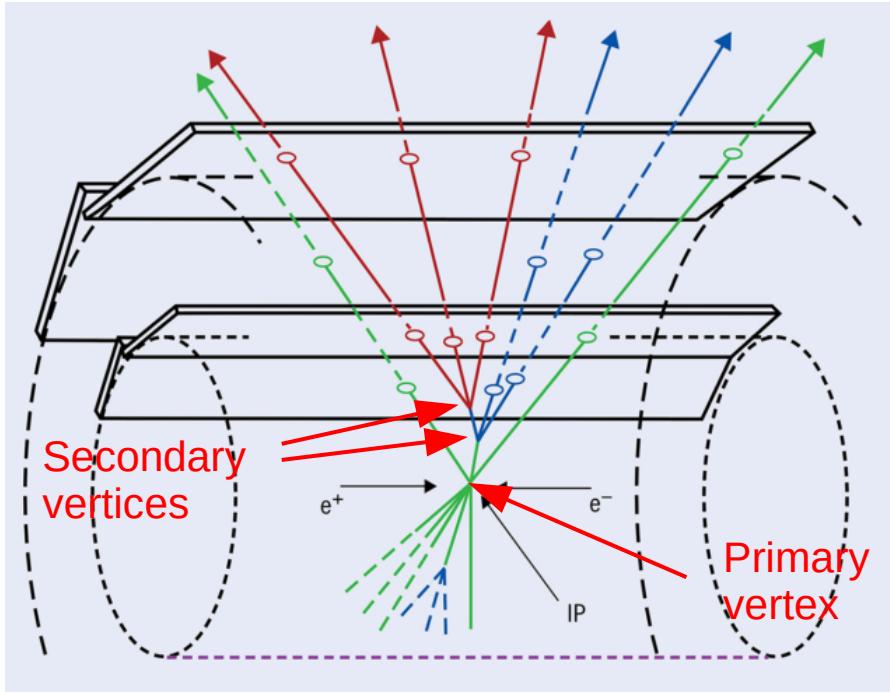
- **ITS Inner Barrel trackets** for the initial primary-vertex reconstruction
- The vertices separated by **~1 mm** are well resolved (may be better, depending on multiplicity)
- This is enough to initiate the standalone ITS tracking

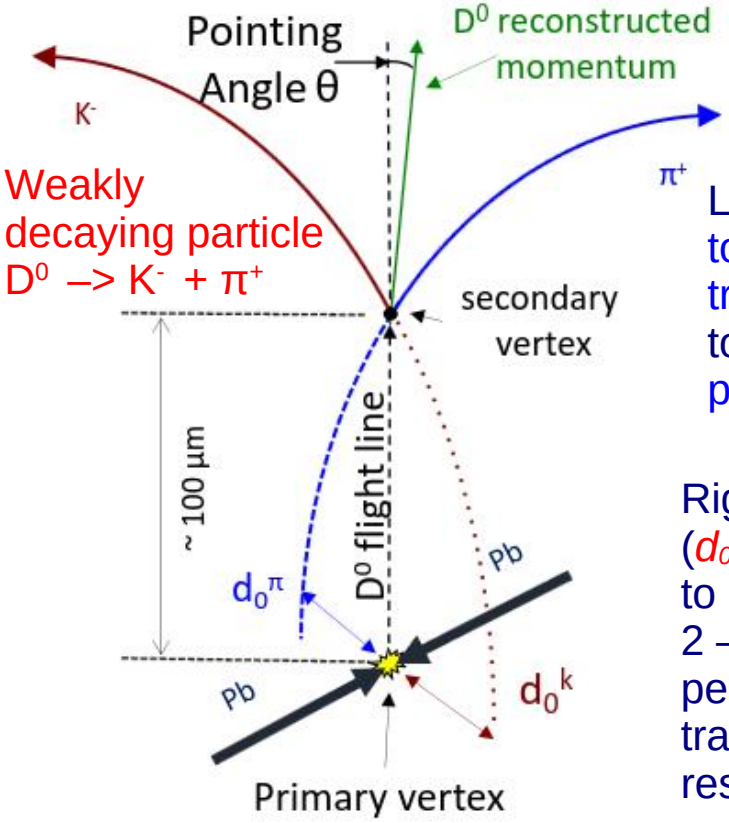


ITS2 event display for one readout frame, for pp collisions at √s = 13.6 TeV. Interaction rate ~1 MHz, timeframe length ~ 5 μs.

Inner Tracking System (ITS2) vertexing performance





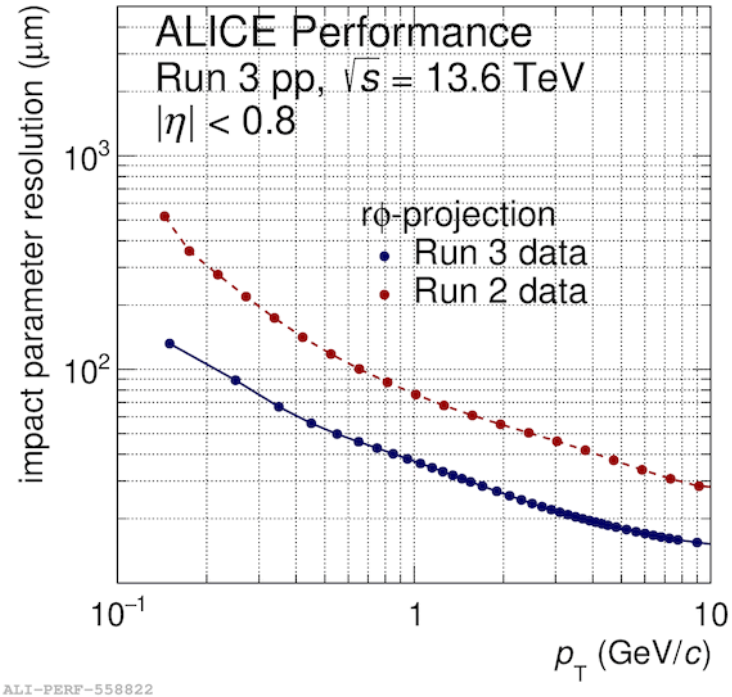


Weakly decaying particle
D^0 –> K^- + π^+

Weak decays –> secondary vertices.

Left: Secondary vertex topology, with daughter track closest approach to primary vertex (impact parameters) d_0^{π} , d_0^{K} .

Right: ITS2 impact parameter (d_0) resolution (blue) compared to old ITS resolution (red). 2 – 3 times improvement, performance depends on transverse momentum p_T, resolution ~ 5 µm at high p_T.



What determines the vertex / impact parameter resolution?

Contributions from intrinsic position resolution:

$$\sigma_{\mathrm{vtx}}^{\mathrm{slope}} \sim \frac{\sqrt{2}\sigma_{\mathrm{int.pos}}}{r_2 - r_1} \cdot \frac{1}{2}(r_1 + r_2); \quad \sigma_{\mathrm{vtx}}^{\mathrm{shift}} \sim \frac{\sqrt{2}}{2}\sigma_{\mathrm{int.pos}}$$

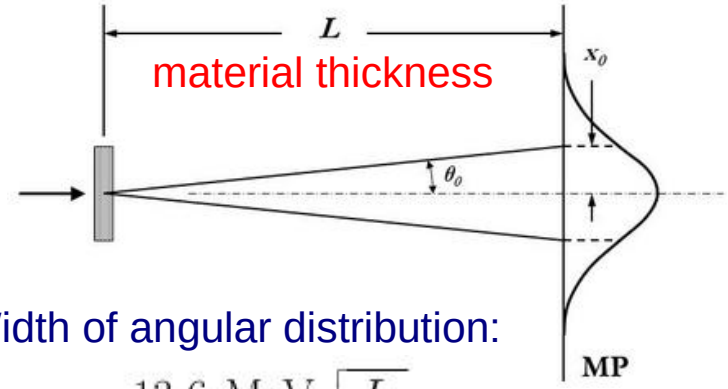
where $\sigma_{int.pos}$ is the intrinsic position resolution.

Adding the two contributions gives:

$$\sigma_{\mathrm{vtx}}^{\mathrm{int.pos}} \sim \sigma_{\mathrm{int.pos}} \cdot \sqrt{\frac{r_1^2 + r_2^2}{(r_2 - r_1)^2}}$$

Depends on vertex (ITS) detector geometry.

From multiple Coulomb scattering of charged particles traversing matter (Leo 2.5):



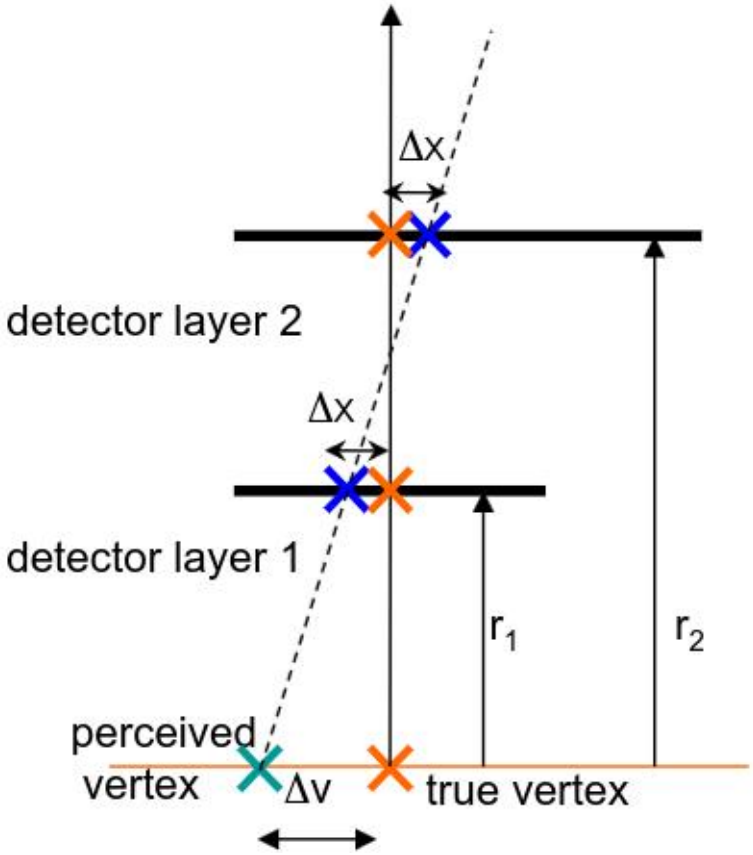
Width of angular distribution:

$$\theta_0 \sim \frac{13.6\ \mathrm{MeV}}{\beta cp}\sqrt{\frac{L}{X_0}}$$

X_0: radiation length
p: momentum

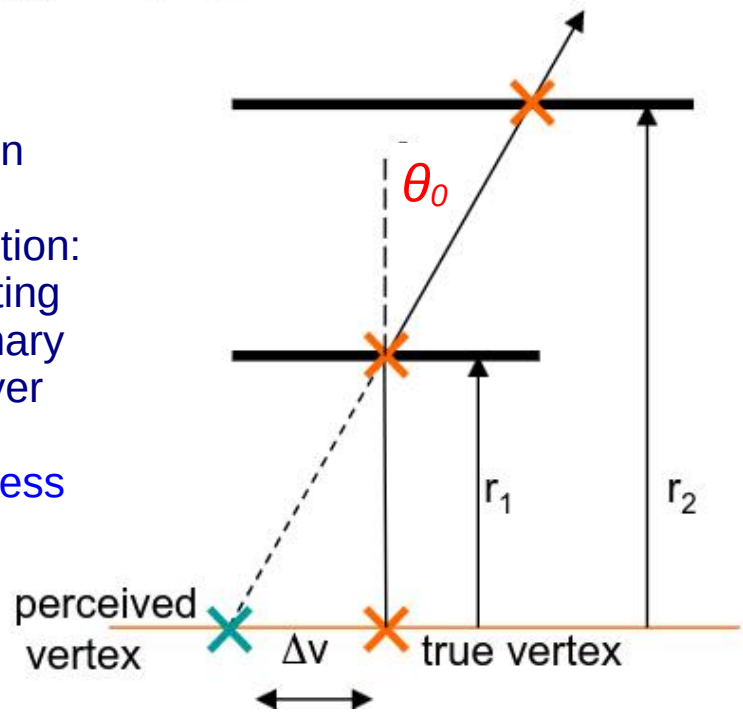
Contribution to vertex resolution:

$$\sigma_{\mathrm{vtx}}^{\mathrm{scatt}} \sim \theta_0 \cdot r_1$$

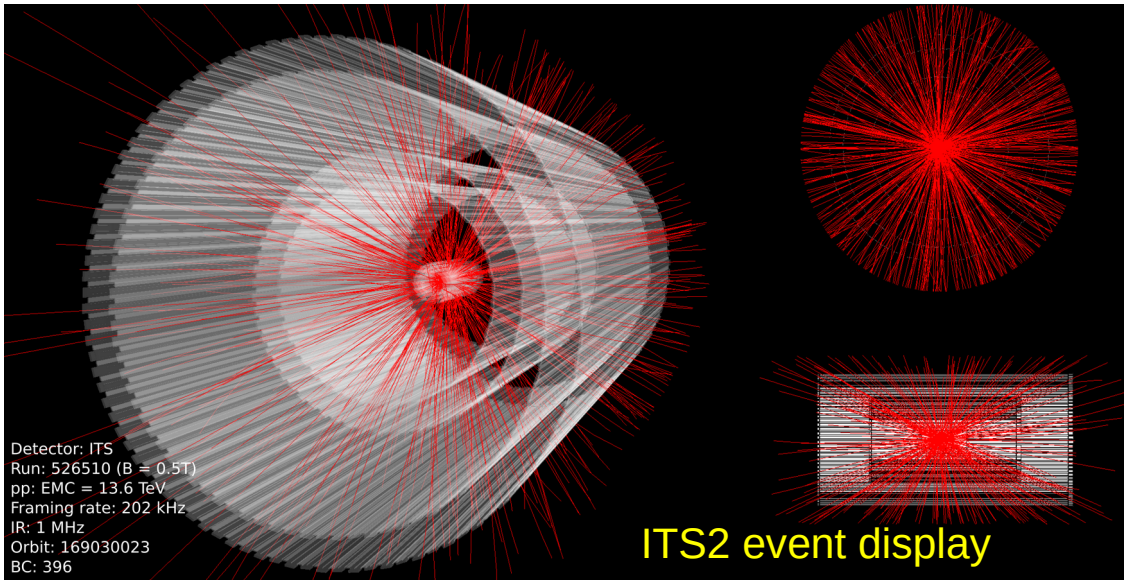


Final vertex resolution:
Add $\sigma_{vtx}^{int.pos.}$ and σ_{vtx}^{scatt} in quadrature.

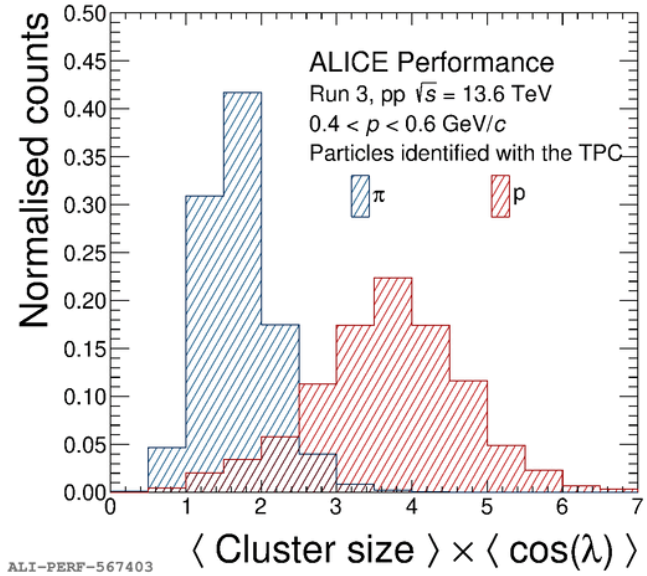
Optimising vertex resolution:
Small radii r_1 and r_2 (getting close to beam line / primary vertex), not too small lever arm ($r_2 - r_1$).
Minimise material thickness L/X_0 in vertex detector.
Better for high p.



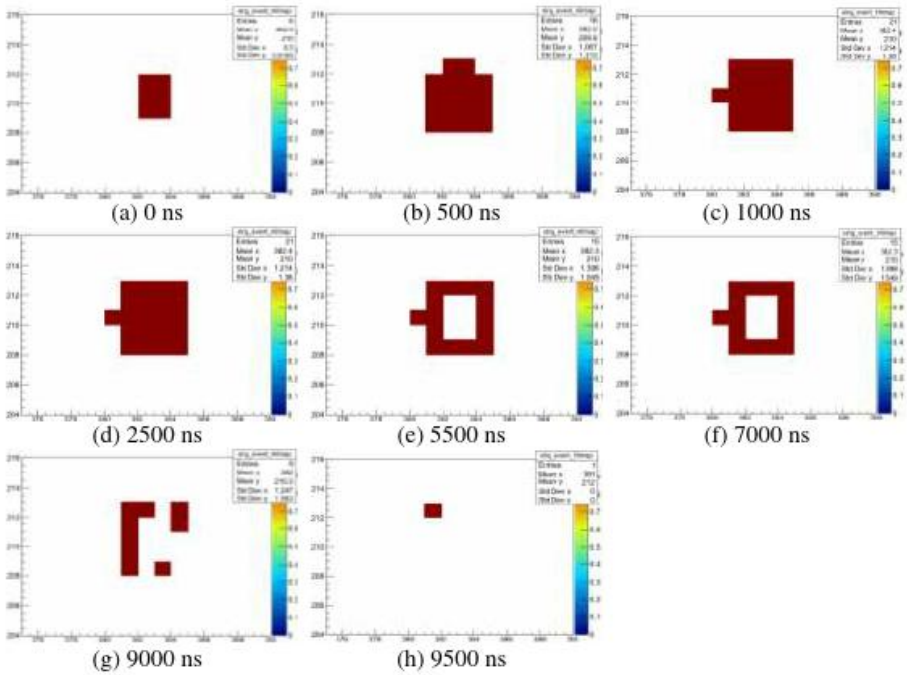
Inner Tracking System (ITS2) PID performance



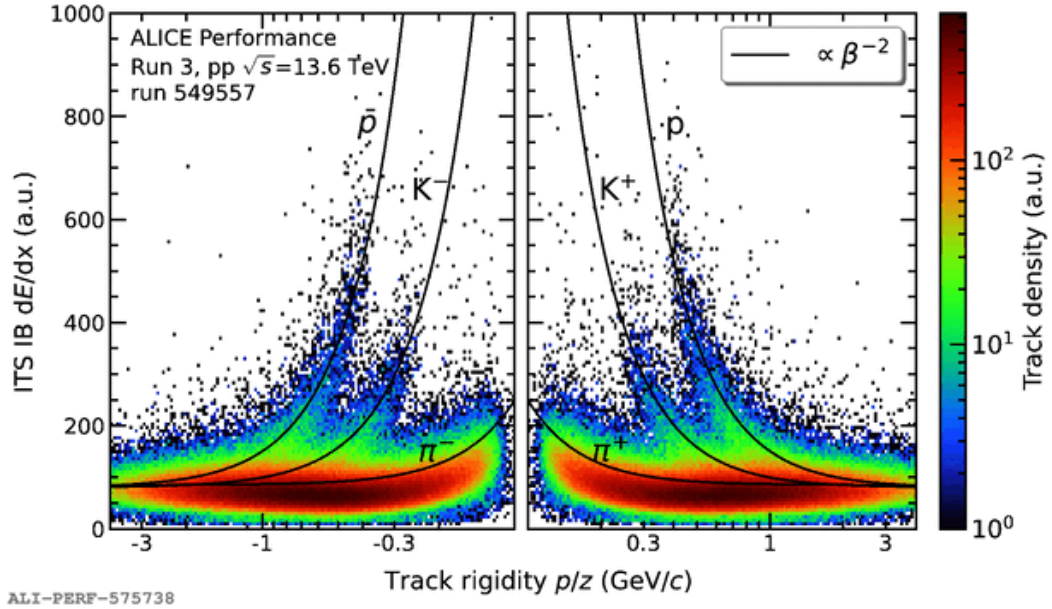
ITS2 p / π separation power based on cluster size (TPC PID)



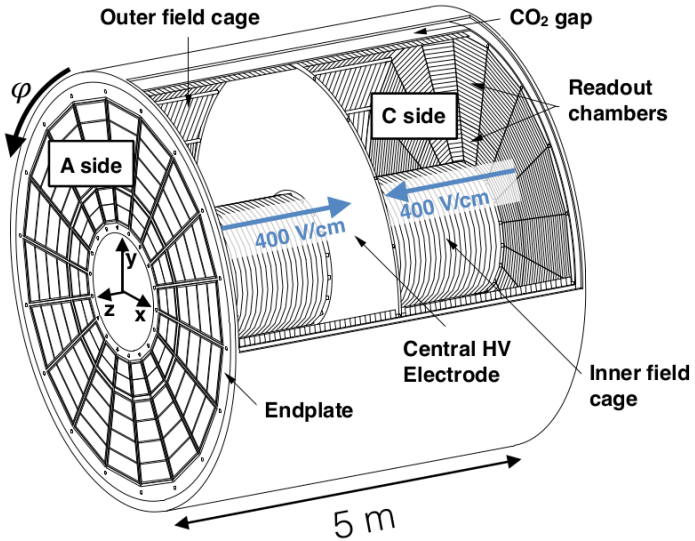
Clusters in ALPIDE chip, measured with ^{241}Am α source, no reverse bias – electrons collected slowly by diffusion, cluster growing transversely with time.



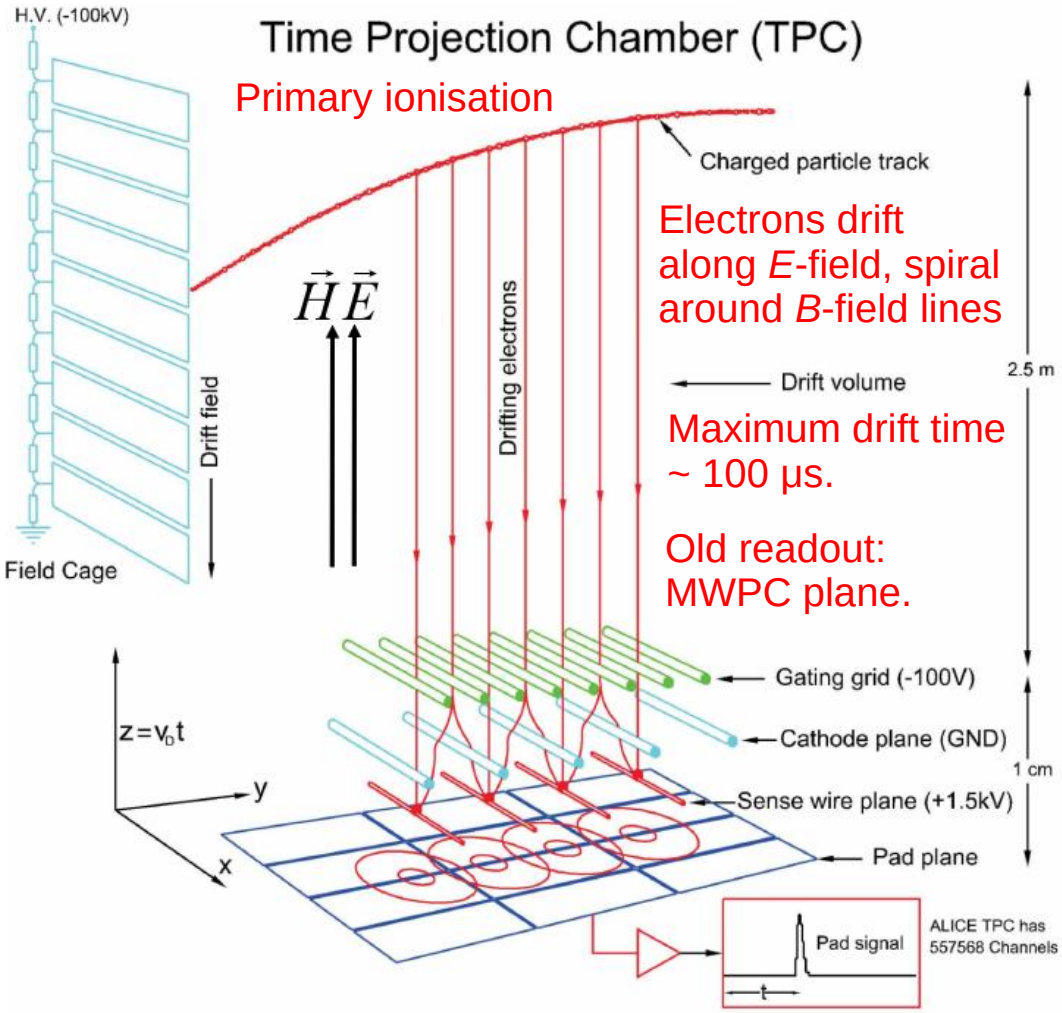
ITS2 PID performance with cluster size and number of consecutive timebins above threshold providing *dE/dx* information.



The ALICE TPC in Run 3



ALICE Time Projection Chamber: Large cylindrical gas ionisation detector, gas mixture 90% Ne, 10% CO_2, 5% N_2.
Drift *E*-field 400 V/cm, *B*-field 0.5 T.
Readout planes at endcaps. 3D spacepoints via (*x*,*y*,*z*) or (*r*,*φ*,*z*) from (padrow, pad number, drift time). Space points found using centre of gravity method.
New endcap readout system in Run 3: Gas Electron Multipliers (GEMs). Micromesh with insulator sandwiched between two electrodes, strong *E*-field in holes.



Electrons drift along *E*-field, spiral around *B*-field lines

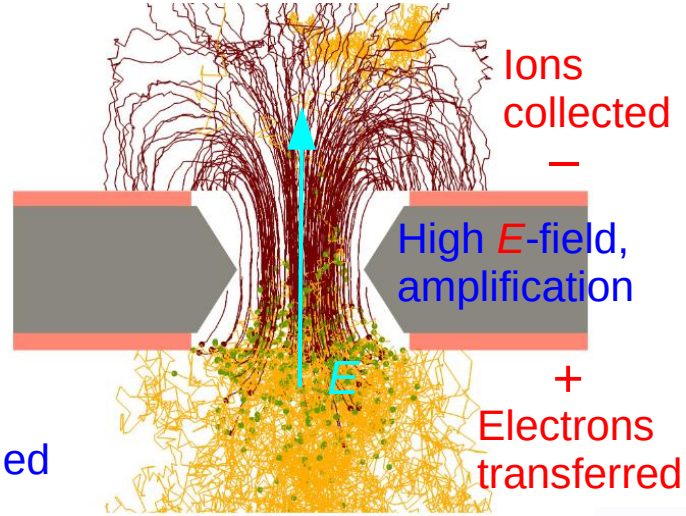
Maximum drift time ~ 100 μs.

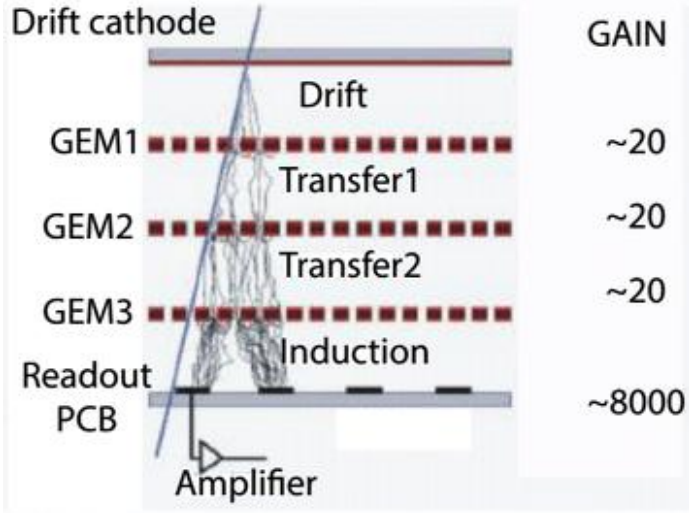
Old readout: MWPC plane.

Ions collected on – side. Little ion buildup in drift volume but still some *E*-field distortion due to high luminosity.

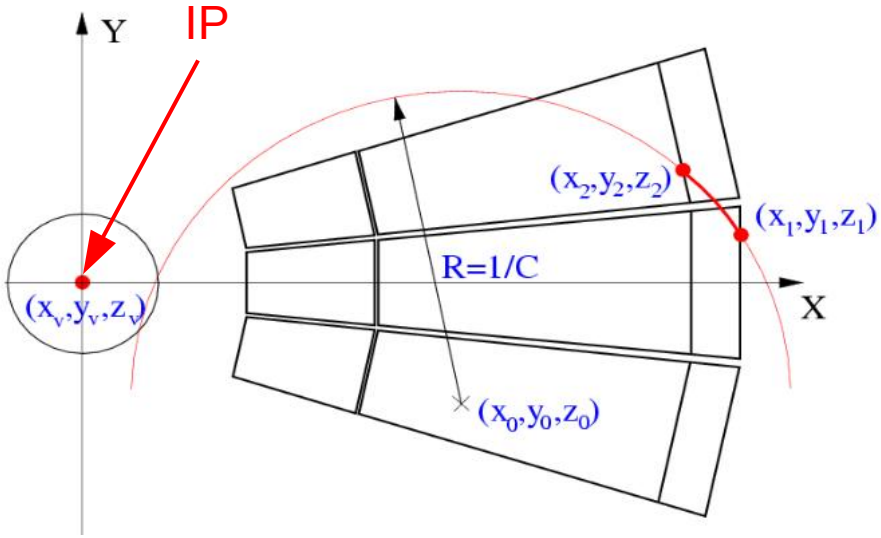
Electrons amplified and transferred, typically several transfer structures.

Very fast, negative signal on pad plane from electron collection.





TPC tracking and PID

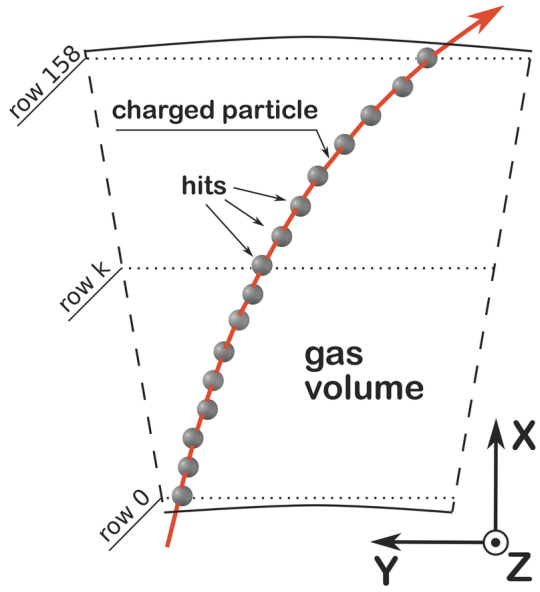


Transverse momentum p_T of particle provided by track curvature R in B-field:

$$p_T = qBR$$

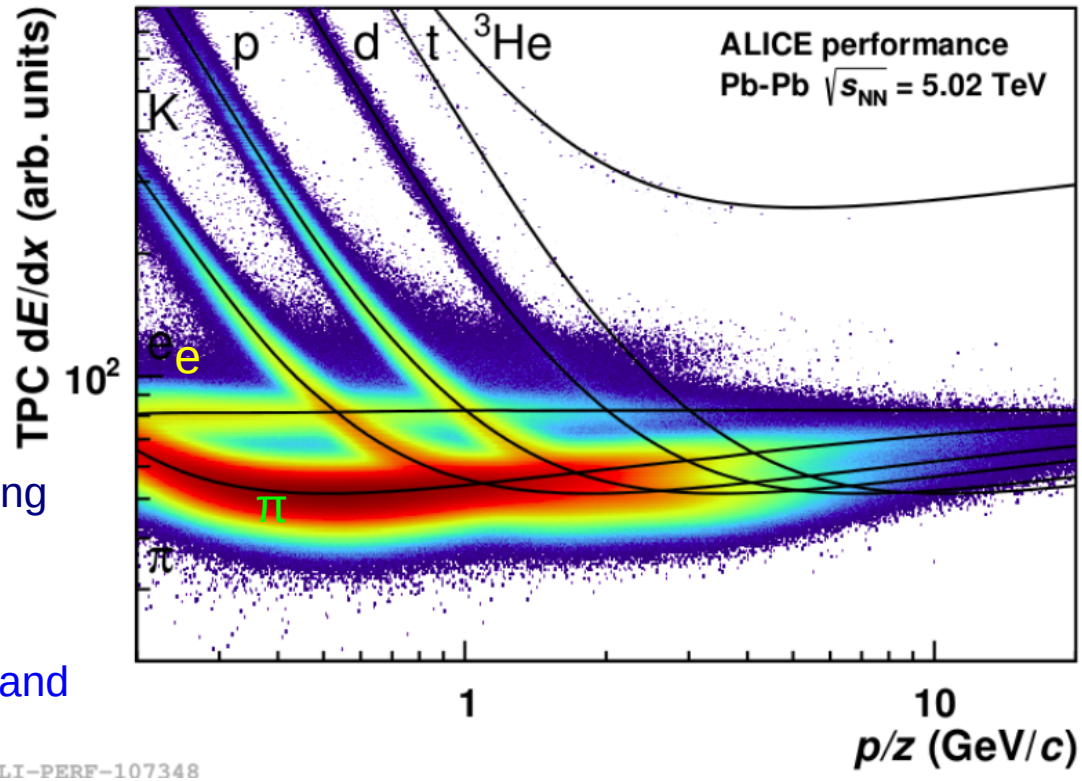
Longitudinal momentum p_L provided by angle θ relative to beam axis:

$$\frac{p_T}{p_L} = \tan\theta$$



Tracking starts from tracklet in outermost padrows, interaction point constraint defines a helical track segment. Tracking proceeds inwards row by row, picking up hits and refining track seed parameters taking space point uncertainties into account (Kalman filter). Best track candidates kept after maximum likelihood fit.

PID information provided by specific energy loss in gas, *dE/dx* (Bethe-Bloch). Large fluctuations (Landau distribution), improve *dE/dx* resolution by keeping only 60% of space points with lowest hit *dE/dx* before computing track <*dE/dx*> –> truncated mean, near-Gaussian distribution.
PID done via parametrised cuts on <*dE/dx*> as functions of *p* for each particle species (inclusion and exclusion cuts), exploiting resolution σ.



ALI-PERF-107348

What determines the track momentum resolution?

Transverse projection of charged particle track in B-field forms an arc of a circle with radius R, related to transverse momentum p_T:

$$p_{\mathrm{T}}\ (\mathrm{GeV}/c) = qBR \sim 0.3BR\ (\mathrm{Tm})$$

Sagitta s of arc depends on radius R:

$$s = R(1-\cos\theta) \sim \frac{1}{2}R\sin^2\theta \sim \frac{1}{2}R\theta^2$$

and on length L between track end and primary vertex:

$$s \sim \frac{1}{8}\frac{L^2}{R} \sim \frac{0.3BL^2}{8p_{\mathrm{T}}}$$

Sagitta defined by at least 3 space points:

$$s = x_2 - (x_1+x_3)/2 \ \rightarrow\ \sigma_s = \sqrt{(3/2)}\sigma_{\mathrm{int.pos}}$$

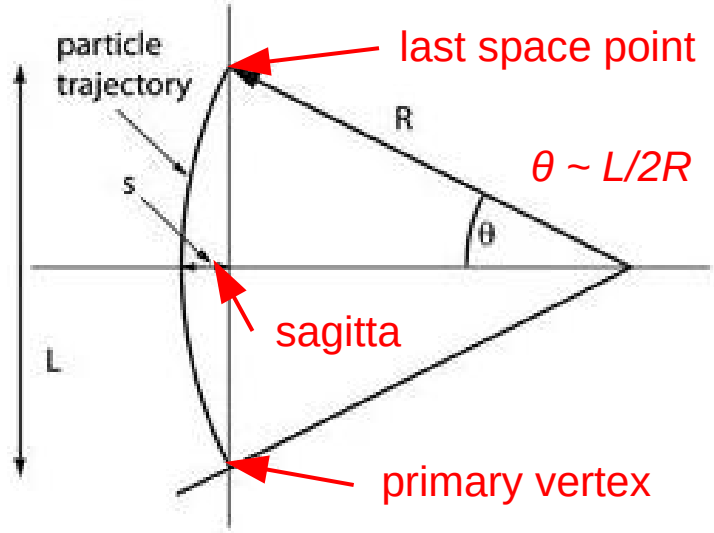
Relative uncertainty in p_T (3 space points):

$$\frac{\sigma_{p_{\mathrm{T}}}}{p_{\mathrm{T}}} = \frac{\sigma_s}{s} \sim \frac{8\sqrt{(3/2)}\ \sigma_{\mathrm{int.pos}}\ p_{\mathrm{T}}}{0.3BL^2}$$

Relative uncertainty in p_T ($N > 10$ space points):

$$\frac{\sigma_{p_{\mathrm{T}}}}{p_{\mathrm{T}}} \sim \frac{\sigma_{\mathrm{int.pos}}\ p_{\mathrm{T}}}{0.3BL^2}\cdot\sqrt{720/(N+4)}$$

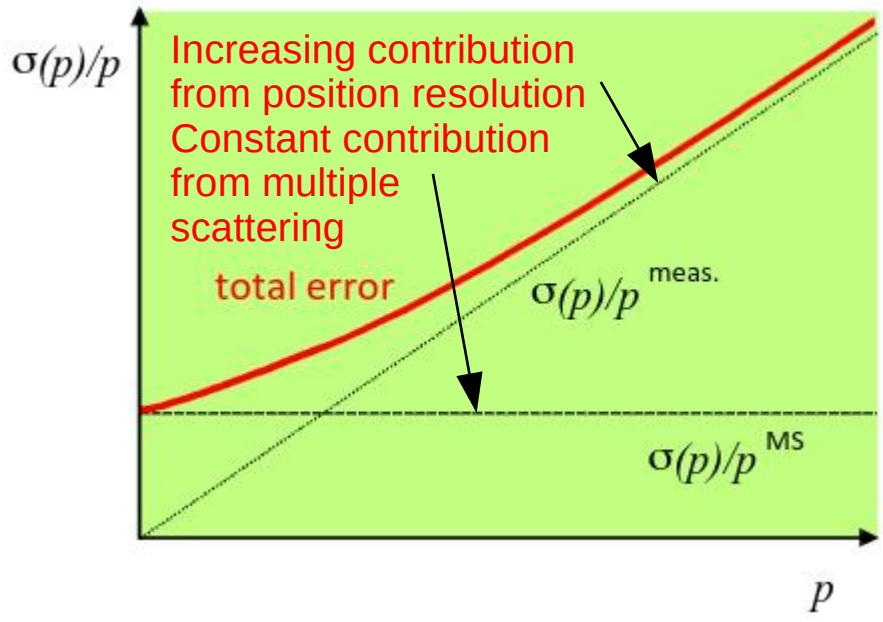
Takeaway message: Relative uncertainty $\sigma_{pT}/\,p_{\mathrm{T}}$ is proportional to p_{T} and to $\sigma_{\mathrm{int.pos}}$, and improves with the number N of measured space points.



Contribution from multiple scattering:

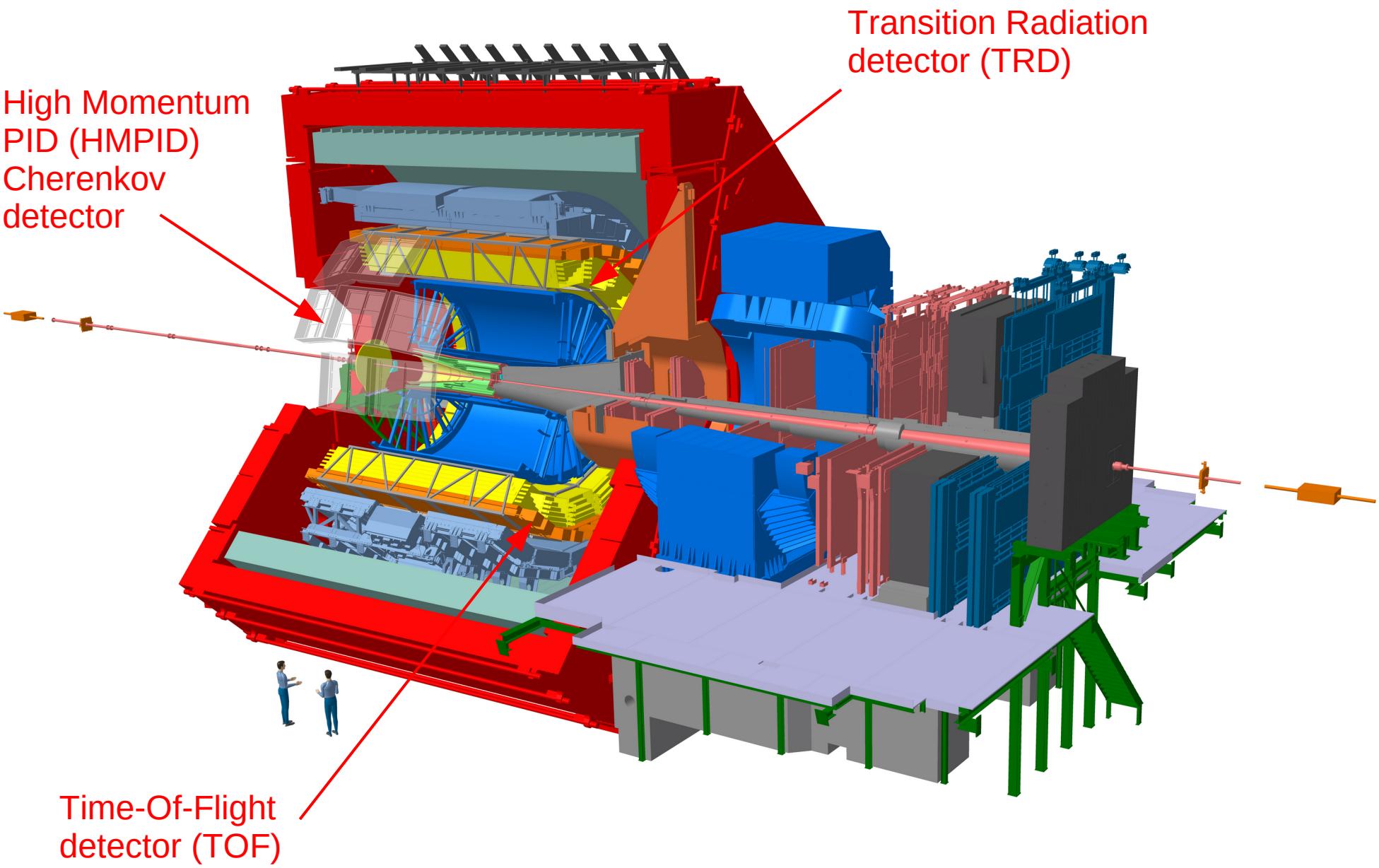
$$\theta_0 \sim \frac{13.6\ \mathrm{MeV}}{\beta cp}\sqrt{\frac{L}{X_0}}\ ;\quad \sigma_s^{\mathrm{scatt}} = L/2\cdot\theta_0$$

which gives a constant $\dfrac{\sigma_{p_{\mathrm{T}}}^{\mathrm{scatt}}}{p_{\mathrm{T}}} \sim \dfrac{0.045\ (\mathrm{T}\cdot\mathrm{m})}{B\sqrt{LX_0}}$

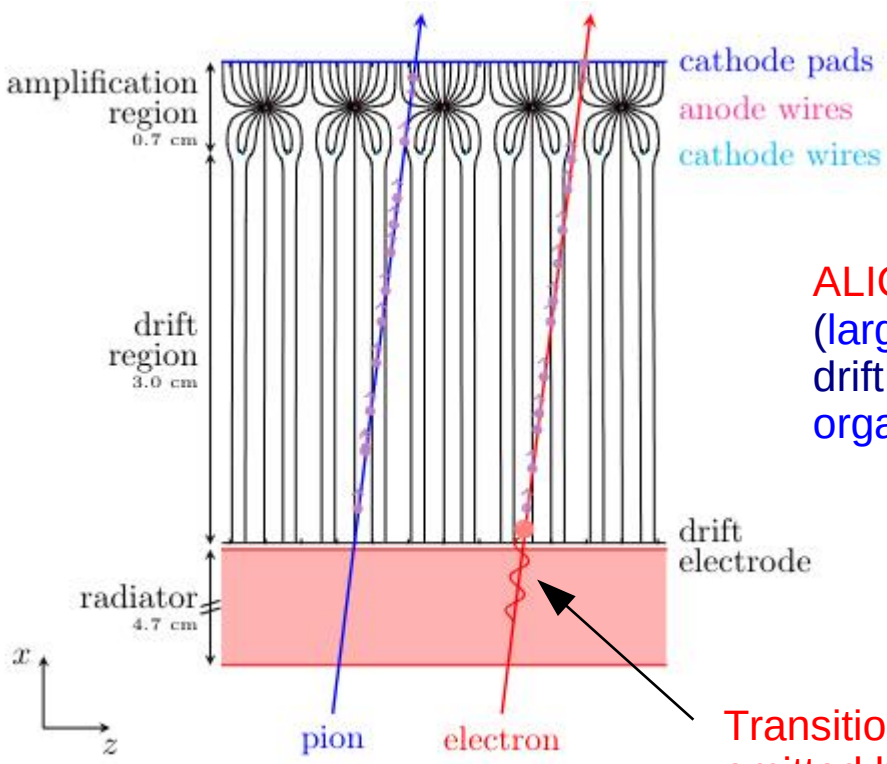


The ALICE detector (Run 3 version)

Central barrel charged particle PID detectors



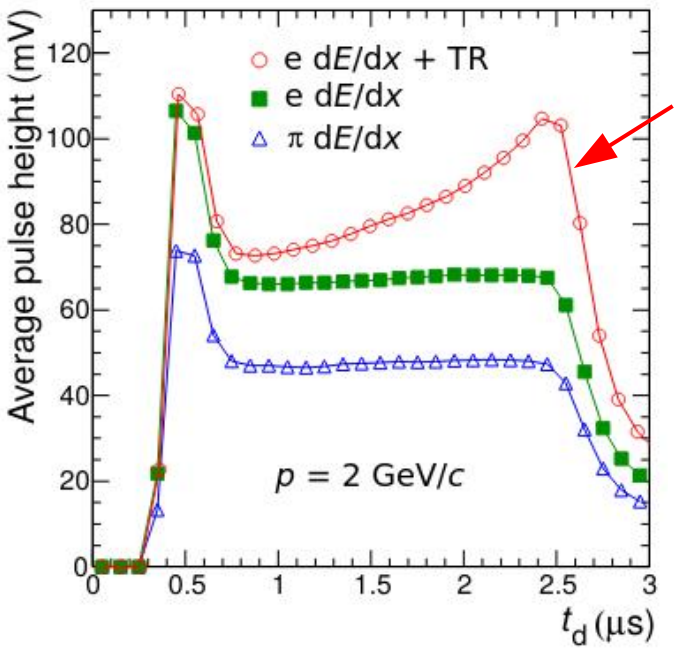
Transition radiation detector



Transition radiation (X-rays) emitted when a particle with Lorentz factor $\gamma = (1 - \beta^2)^{-1/2} > 10^3$ crosses the boundary between media with different dielectric constants. Helps electron identification.

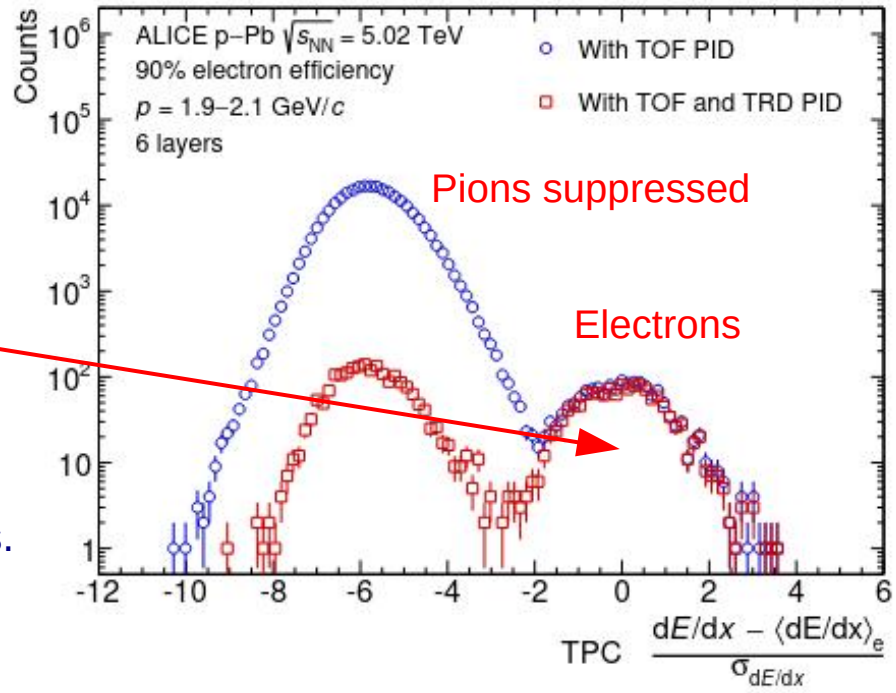
ALICE TRD: MWPC with a Xe (85%), CO_2 (15%) gas mixture (large Z, good for absorbing X-rays), with a 3 cm drift region, drift field 700 V/cm. Preceded by a radiator of sandwiched organic foam / fibre material. 6 MWPC layers surrounding TPC.

ALICE TRD: Fast detector with fast online reconstruction of tracklets, providing "rare signal" triggers for electrons and high-p_T particles. Extra space points for improving p_T resolution of central barrel tracking.

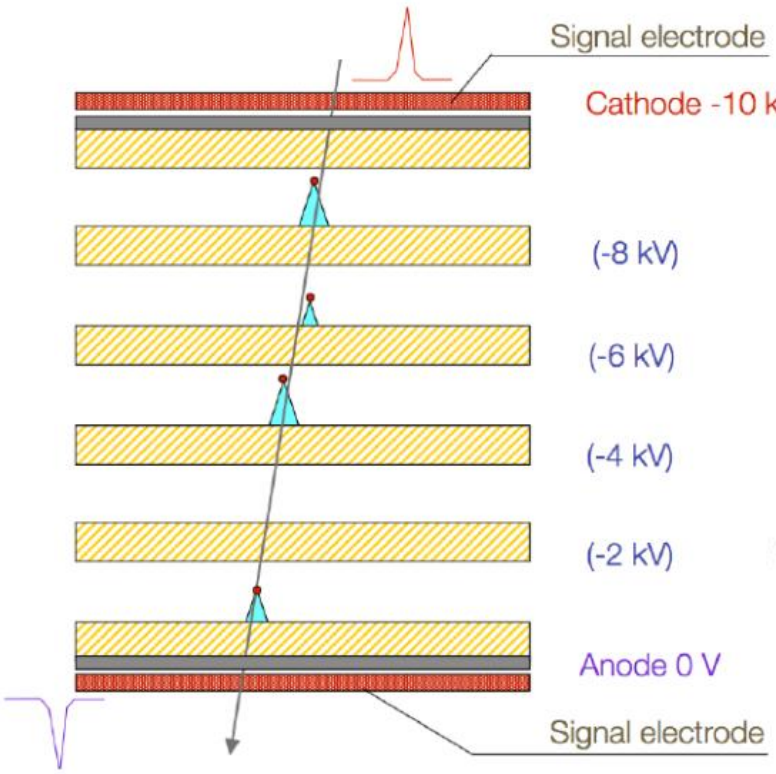


Energy deposit *dE/dx* vs drift time: TR from electrons arrives late (long drift distance).

Electron identification using TRD time information selects a very pure electron sample, rejecting pions.



Time-of-flight detector



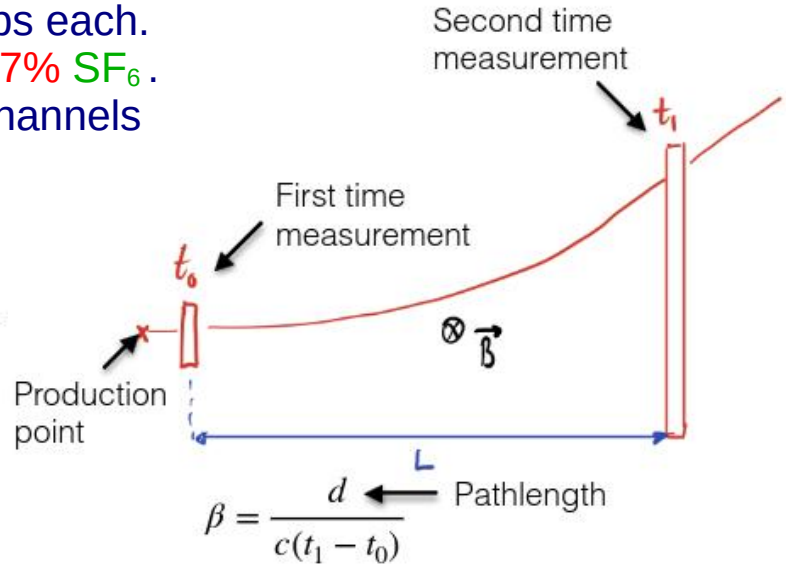
ALICE Time-of-flight detector: Based on Multigap Resistive Plate Chamber technology. Gas detector operated in avalanche mode. HV applied to external electrodes, internal plates (glass) electrically floating and transparent to (very fast) signal.

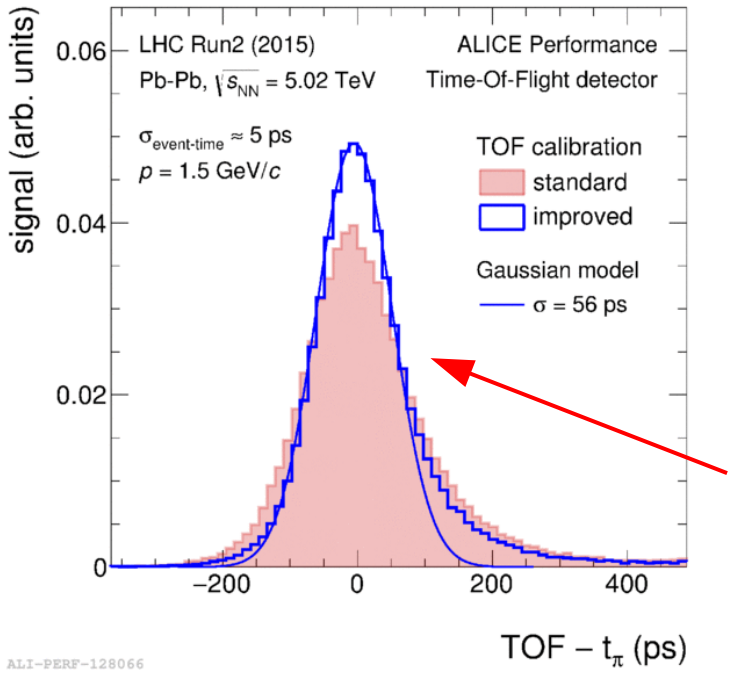
2 stacks with 5 250 µm gaps each.
Gas mixture 93% $C_2H_2F_2$, 7% SF_6.
High granularity, 157248 channels (3.5 x 2.5 cm^2).

Quantity used for PID:

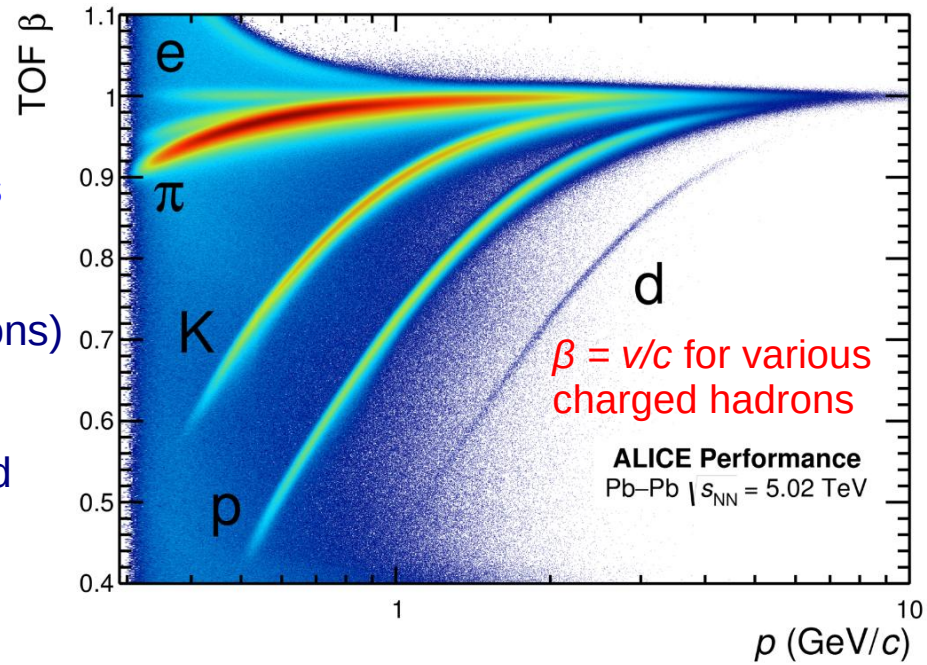
$$n_\sigma = \frac{t_{\mathrm{TOF}} - t_{\mathrm{event}} - t_{\mathrm{track},i}}{\sigma_{\mathrm{tot}}}$$

t_{TOF}: measured time for matched track
t_{event}: event time, from dedicated detector (FT0) or from average arrival of high-p_T particles
$t_{track,i}$: expected flight time for mass hypothesis i
σ_{tot}: time resolution (several contributions)



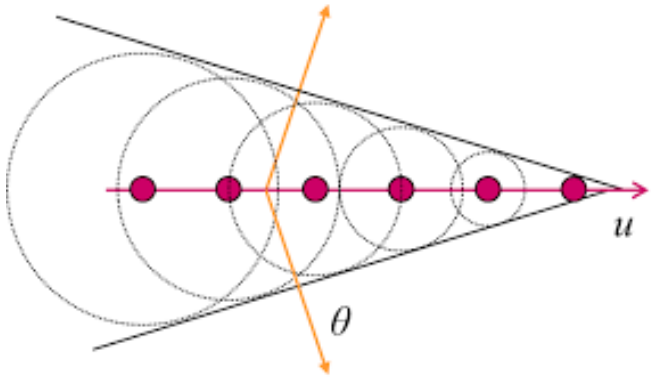


TOF resolution σ_{tot} : ~ 56 ps with improved calibration.



ALI-PERF-128066

Cherenkov detector

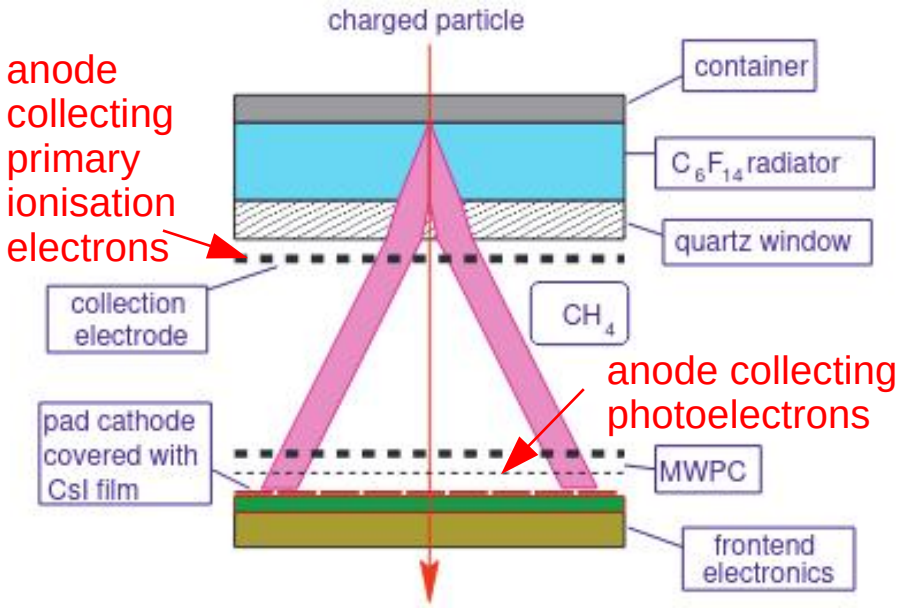


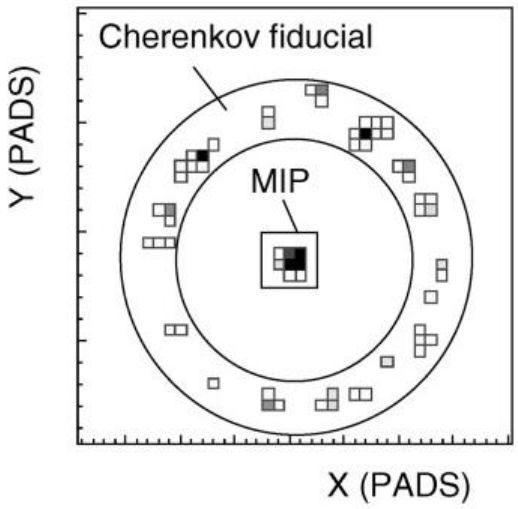
Cherenkov light (UV) is emitted when charged particle speed in a medium exceeds $\beta = v/c > 1/n$, in cone with opening angle θ given by:
Here n is the medium index of refraction.

$$\cos\theta = \frac{1}{\beta n}$$

ALICE HMPID detector: Liquid C_6F_{14} radiator (n = 1.299 for λ = 175 nm). Photons propagate through CH_4 to MWPC readout plane with photocathode pads coated with CsI –> photoelectrons initiate avalanches. UV photons reaching readout plane form a circular pattern, normal dE/dx from traversing MIP in ring centre. Ring radius R provides opening angle θ –> particle β.

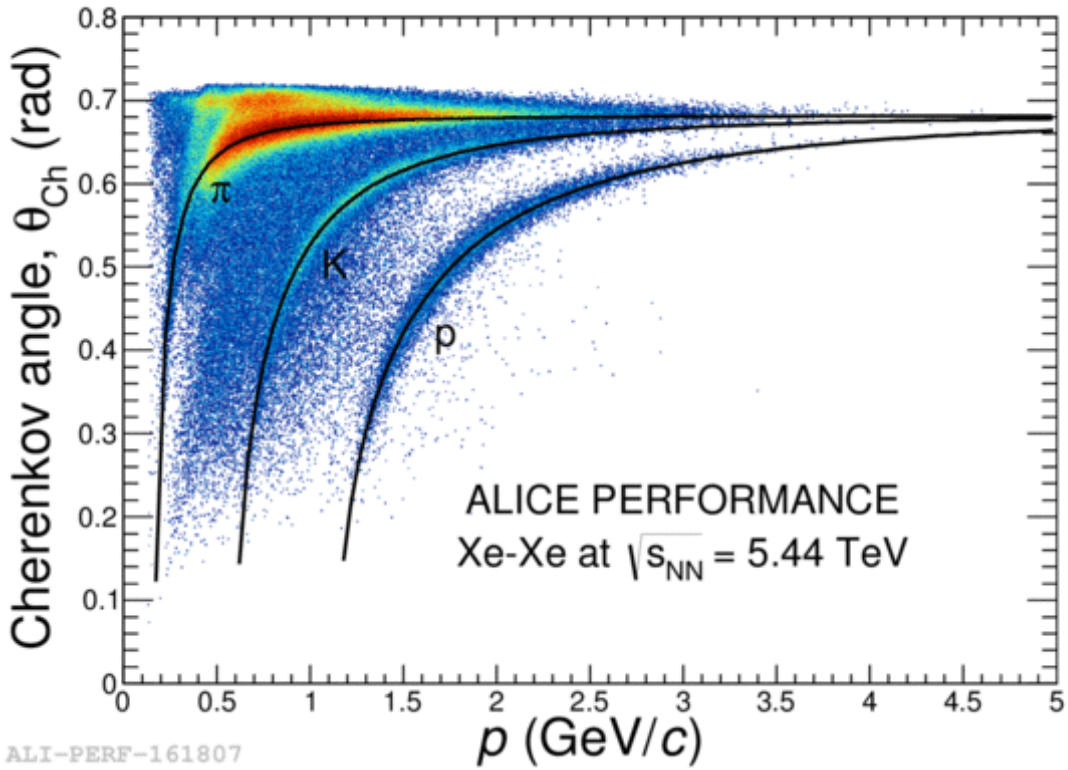
PID again obtained using parametrised cuts exploiting resolution σ.





Cathode pad pitch: ~ 8 x 8 mm^2

Pad hit pattern from Cherenkov photons (ring) and MIP (centre)



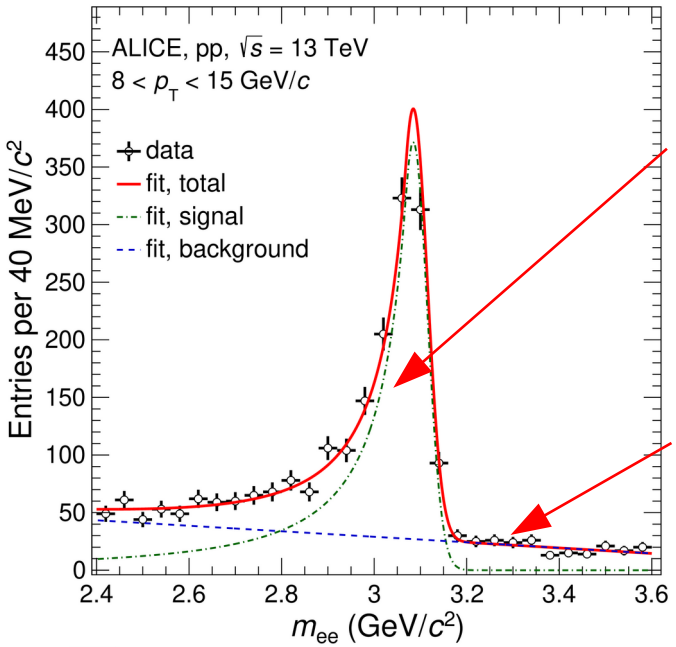
Identification of short-lived particles: Invariant mass

Short-lived particles, decaying before leaving their signature in tracking and PID detectors, must be reconstructed and identified via the invariant mass of their decay products. For a 2-body decay the invariant mass *m* is given as:

$$m^2 = m_1^2 + m_2^2 + 2(E_1 E_2 - \vec{p_1} \cdot \vec{p_2})$$

where (m_1, m_2), (E_1, E_2) and (p_1, p_2) are the rest masses, energies and momentum vectors of the known daughters. For a charged daughter particle, momentum is extracted from track curvature in a *B*-field and mass is obtained using PID techniques. Candidates are histogrammed vs invariant mass and yield is extracted on statistical basis.

Typical example – electromagnetic decay of the charmonium state J/ψ ($c\bar{c}$) –> $e^+ e^-$:



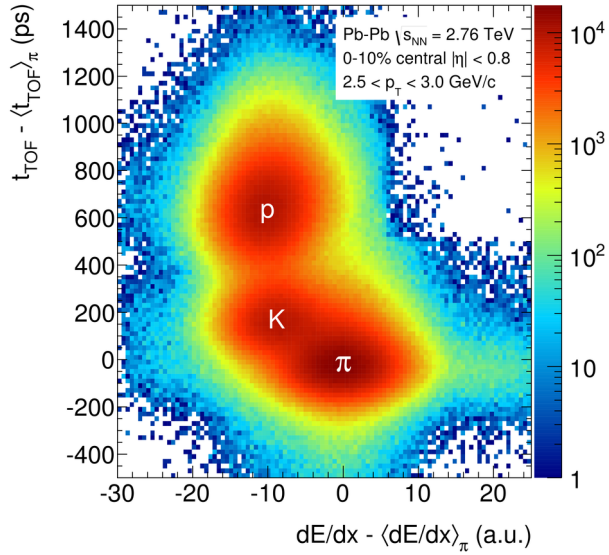
Signal – true J/ψ dielectrons

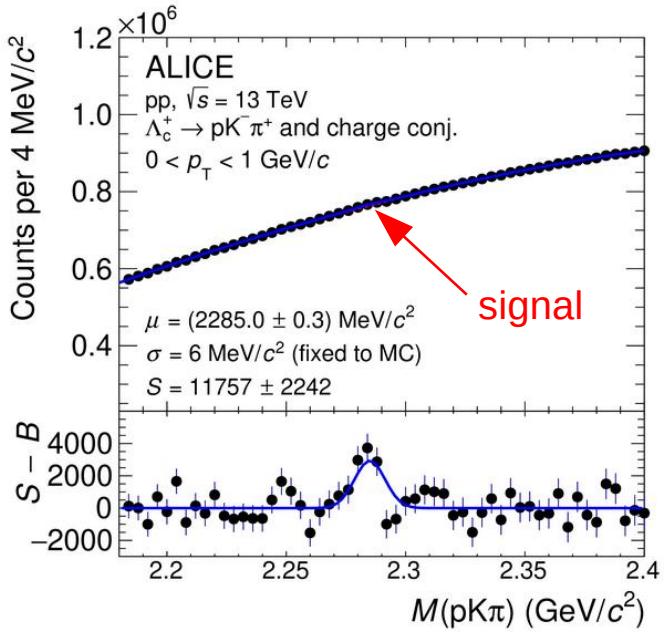
Combinatorial background of unrelated $e^+ e^-$ pairs

Decay topologies can be very complicated. In a more general case (*n*-prong decay, *n* tracks originating from common secondary vertex):

$$m^2_{n-\mathrm{prong}} = \Sigma_i(m_i^2) + 2\Sigma_{i,j\neq i}(E_i E_j - \vec{p_i} \cdot \vec{p_j}))$$

Combinations of PID techniques may be needed to identify daughters (here: TPC *dE/dx* + TOF)





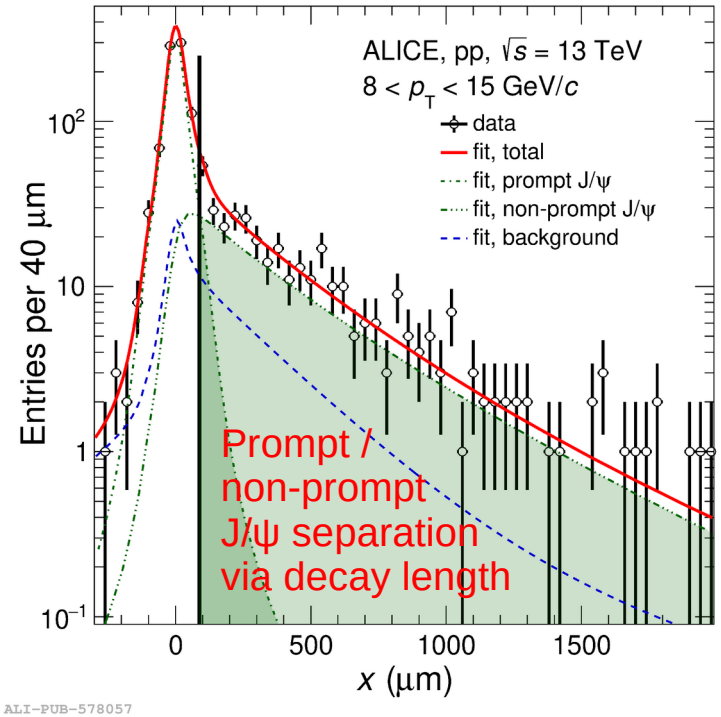
Example of 3-prong decay: Λ_c^+ (usc) –> $p + K^- + \pi^+$ (here: low p_T, very large combinatorial background from unrelated pKπ triplets).

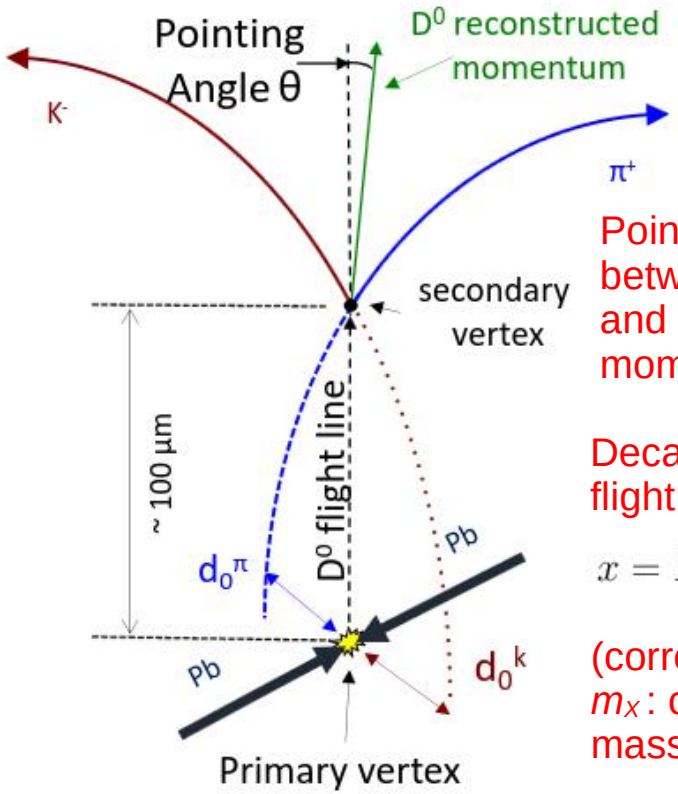
ALI-PUB-578052

Heavy flavour measurements

Open charm and beauty hadrons consist of c (b) quarks combined with u,d,s (u,d,s,c) quarks, and decay weakly, with typical decay lengths $c\tau$ ~ 100 µm (c) and ~ 500 µm (b) and characteristic displaced vertex topologies.
Example: D^0 ($c\bar{u}$) –> $K^- + \pi^+$ ($c\tau$ = 123 µm)

Reconstruction from more long-lived daughter tracks.
Selection of candidates based on topological variables:
– Daughter impact parameters d_0^K and d_0^π (> cut value)
– Often: Daughter PID information
Secondary vertex reconstructed from closest approach of daughter tracks –> can now calculate:
– Candidate pseudoproper decay length x
– Candidate pointing angle θ





Pointing angle θ between flight line and candidate momentum vector

Decay length x from flight line projection L_{xy}:

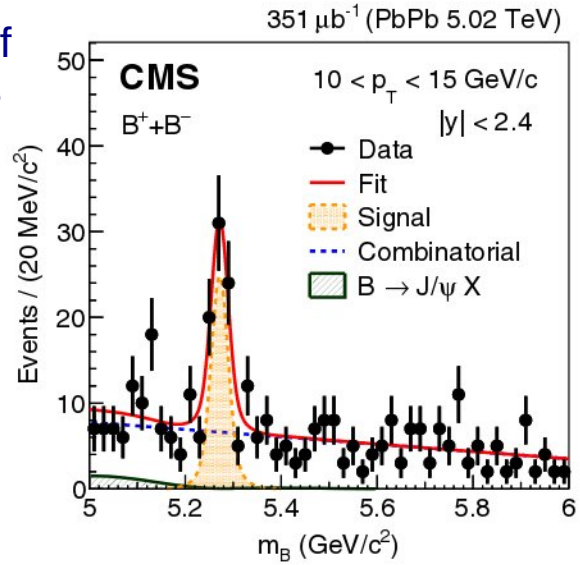
$$x = L_{xy} \cdot c \cdot \frac{m_X}{p_{T,X}}$$

(correct for time dilation)
m_X: candidate rest mass hypothesis

Hidden charm and beauty ($c\bar{c}$, $b\bar{b}$ mesons) are reconstructed in dielectron / dimuon channels. Charmonium state J/ψ also major decay product of B hadrons (non-prompt J/ψ).

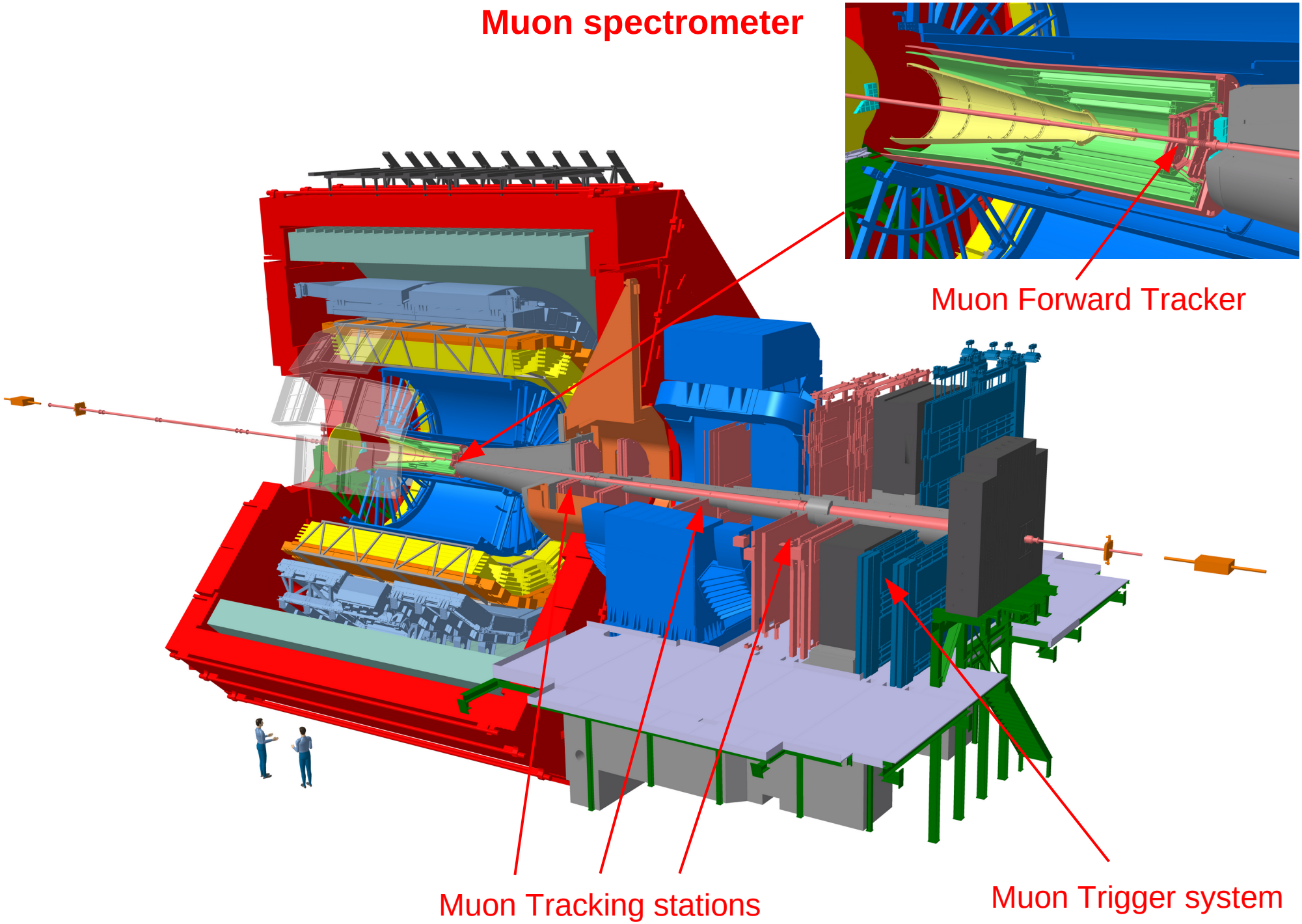
Full reconstruction of rare signals requires invariant mass. Machine learning techniques often involved!

B^{+-} –> J/ψ + K^{+-} invariant mass (CMS)



The ALICE detector (Run 3 version)

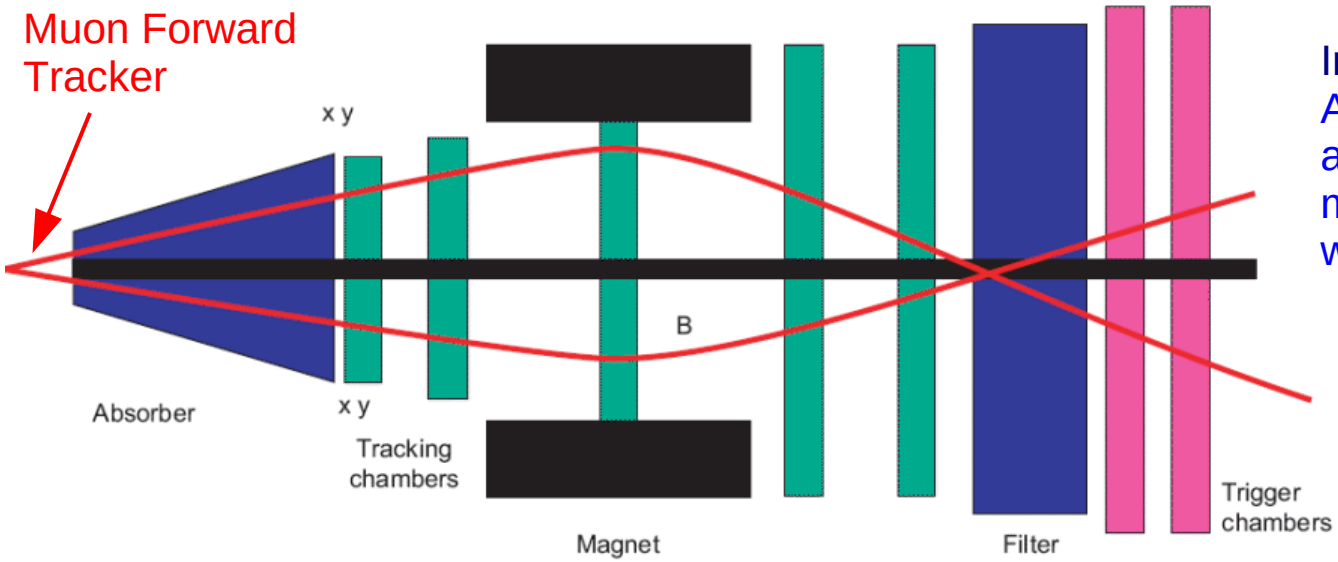
Muon spectrometer



Muon spectrometer

Muons: Very penetrating particles, remain MIPs through thick layers of material.

In order to filter out hadrons, the ALICE Muon Spectrometer has an absorber of concrete in front of the muon tracking chambers, and an iron wall in front of the trigger chambers.

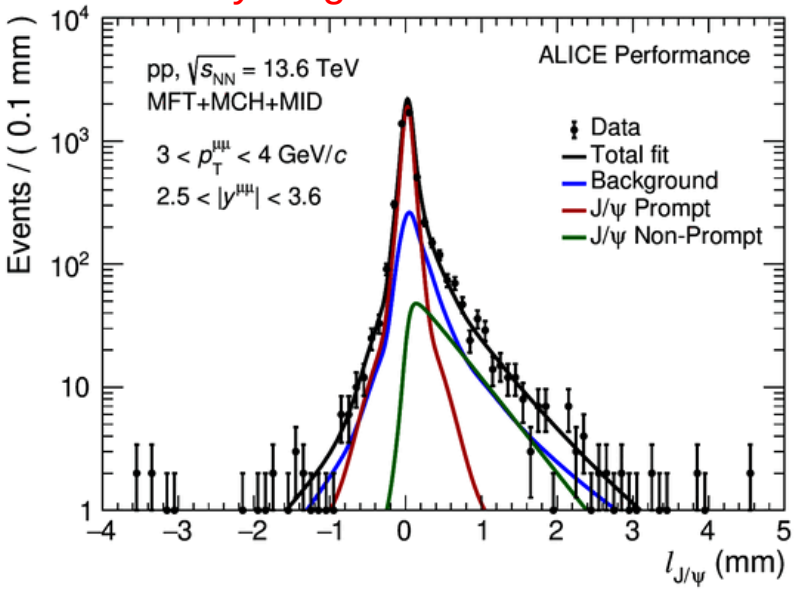


Tracking chambers: 5 stations of MWPC cathode pad chambers (providing *x-y* information), 2 before, 2 after and 1 inside dipole magnet providing momentum *p* measurement.

Run 3 upgrade: Muon Forward Tracker, placed between collision point and absorber. 5 Si pixel planes (ALPIDE) to separate prompt / non-prompt muon pairs (charm / beauty).

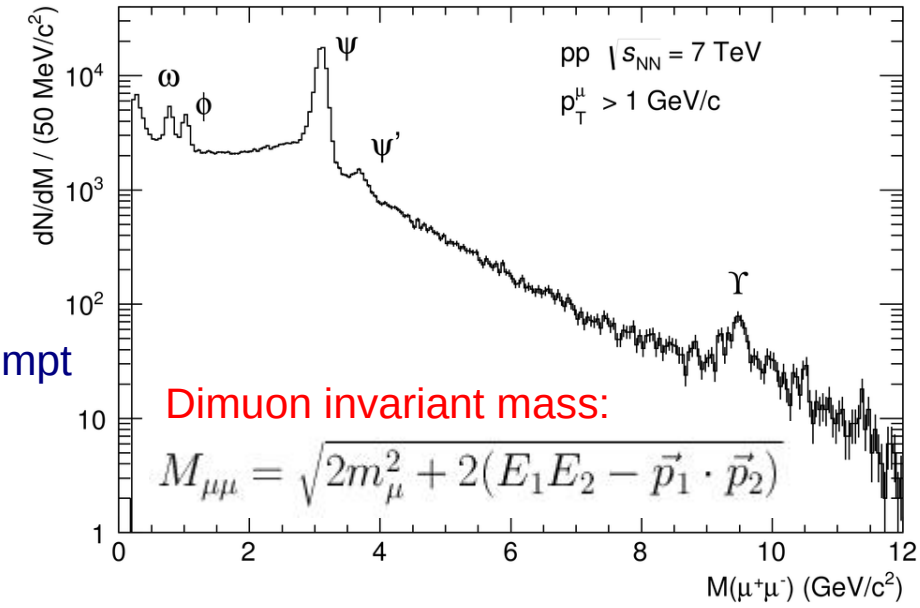
Trigger chambers (now Muon Identifiers): 2 stations of Resistive Plate Chambers, also providing fast momentum estimate.

Decay length distribution



Performance of MFT: Distance primary to secondary vertex for J/ψ in dimuon channel, with prompt / non-prompt separation.

Quarkonia measured in the dimuon channel

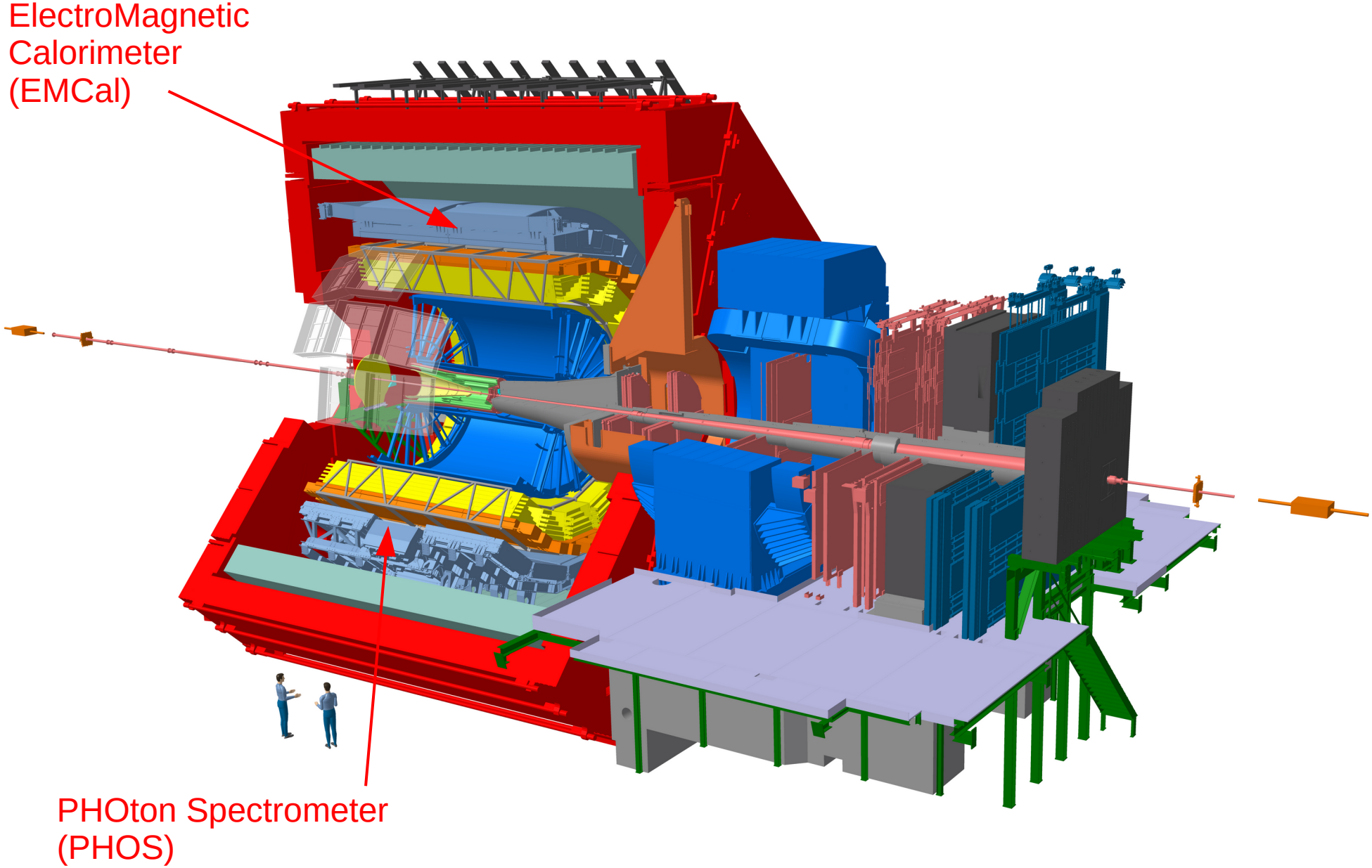


Dimuon invariant mass:

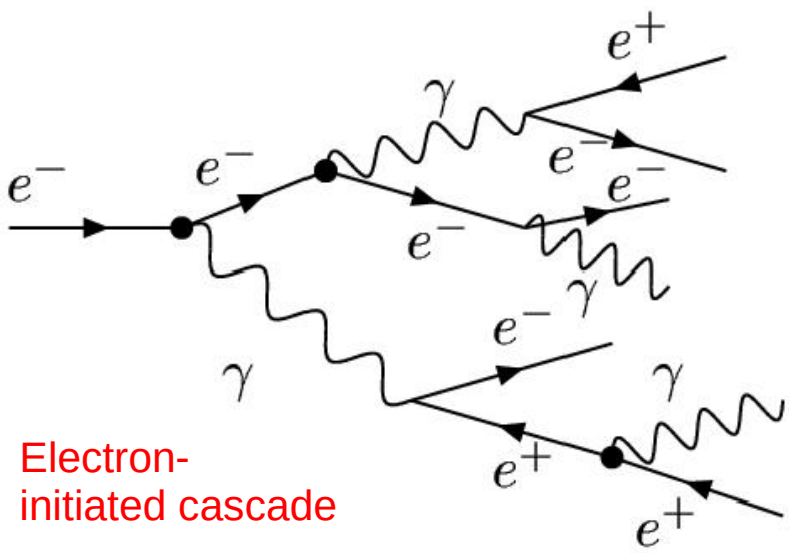
$$M_{\mu\mu} = \sqrt{2m_\mu^2 + 2(E_1E_2 - \vec{p}_1 \cdot \vec{p}_2)}$$

The ALICE detector (Run 3 version)

Central barrel electromagnetic calorimeters
(catching energy of electromagnetic cascade)

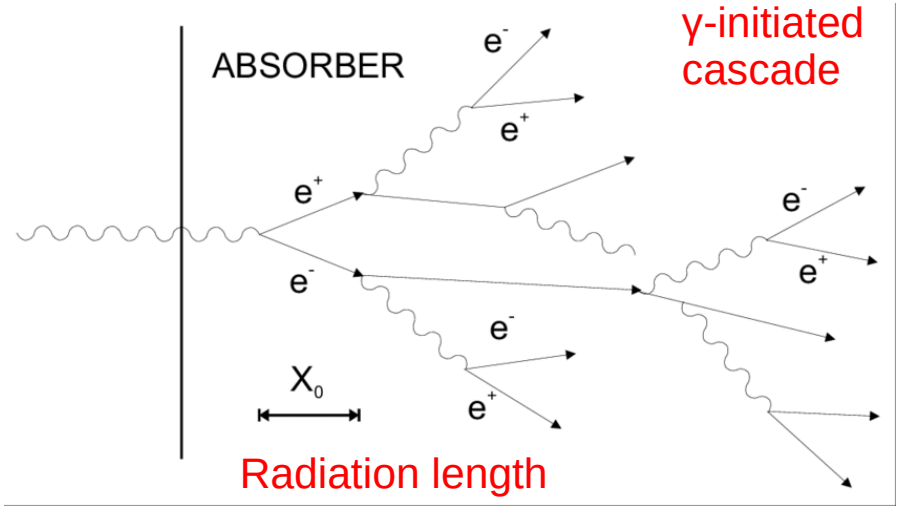


Calorimetry: Electromagnetic cascades



Electron-initiated cascade

Successive steps of electrons / positrons emitting bremsstrahlung and photons absorbed by pair production –> multiplication of particles.



γ-initiated cascade

Radiation length

Critical energy E_c (radiational loss = collisional loss):

$$E_c \sim \frac{800\ \text{MeV}}{Z + 1.2}$$

Radiation length X_0 (distance where E_e –> E_e/e due to radiational loss); ~ typical length λ_{pair} for photon pair production:

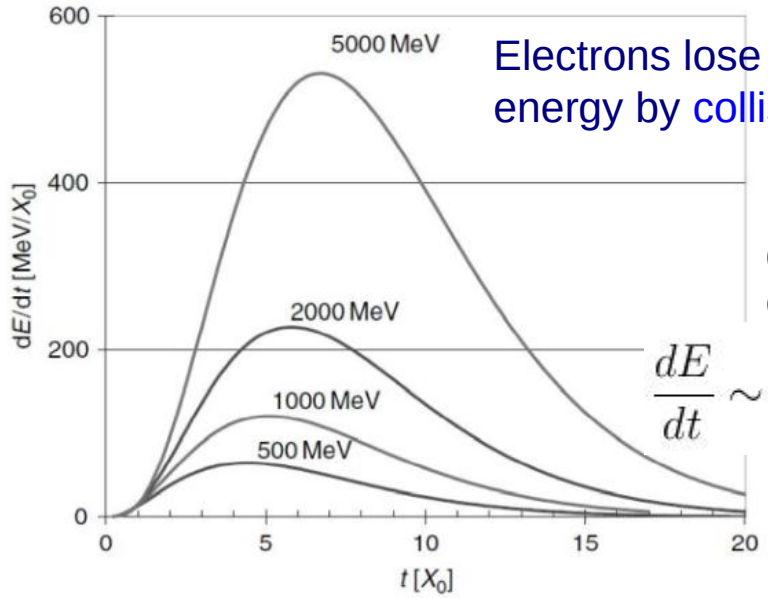
$$X_0 (= L_{rad}) \sim \frac{716.4\ \text{g/cm}^2 A}{Z(Z+1)\ln(287/\sqrt{Z})};\ \ \lambda_{pair} = \frac{9}{7} X_0$$

Initial energy E_0 –> after t radiation lengths there are N particles with energy $E(t)$:

$$N(t) \sim 2^t;\quad E(t) = \frac{E_0}{2^t}$$

Cascade multiplication stops when $E \sim E_c$:

$$E(t_{max}) \sim E_c;\ \ t_{max} \sim \frac{\ln(E_0/E_c)}{\ln 2};\quad N(t_{max}) \sim \frac{E_0}{E_c}$$



Electrons lose remaining energy by collisional loss.

Longitudinal development of cascade:

$$\frac{dE}{dt} \sim E_0 t^{\alpha} \exp(-\beta t)$$

Homogeneous electromagnetic calorimeters

Longitudinal development of cascade depends on radiation length X_0:

$$X_0 (= L_{rad}) \sim \frac{716.4\ \mathrm{g/cm^2} A}{Z(Z+1)\ln(287/\sqrt{Z})};\quad \lambda_{pair} = \frac{9}{7} X_0$$

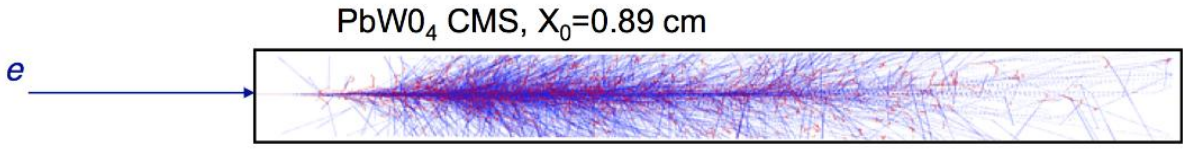
Transverse extent depends on Moliere radius R_M:

$$R_M = X_0 \frac{21.2\ \mathrm{MeV}}{E_c}$$

> 90% of shower deposited within $R = 2\ R_M$

Homogeneous EM calorimeters typically constructed from scintillating material with high Z, for good containment of cascade:

	NaI(Tl)	BGO	CsI(Tl)	$PbWO_4$
density (g/cm^3)	3.67	7.13	4.53	8.28
X_0 (cm)	2.59	1.12	1.85	0.89
R_M (cm)	4.5	2.4	3.8	2.2
dE/dx_{mip} (MeV/cm)	4.8	9.2	5.6	13.0
light yield (photons/MeV)	$4 \cdot 10^4$	$8 \cdot 10^3$	$5 \cdot 10^4$	$3 \cdot 10^2$
energy resolution σ_E/E	$1\%/\sqrt{E}$	$1\%/\sqrt{E}$	$1.3\%/\sqrt{E}$	$2.5\%/\sqrt{E}$



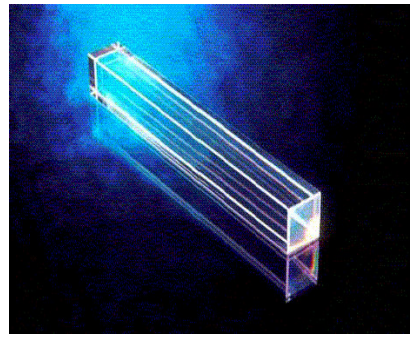
Resolution of homogeneous calorimeter:

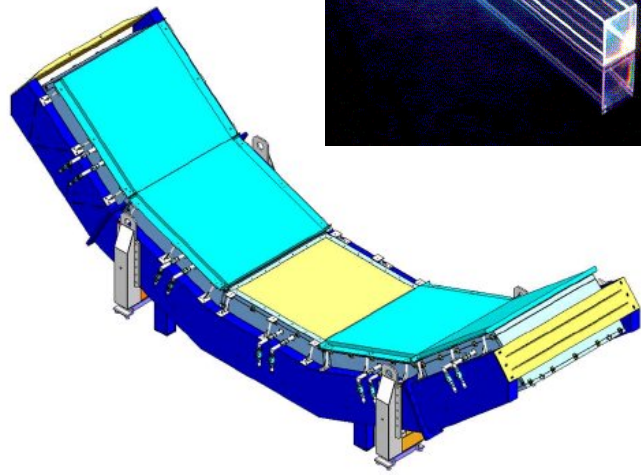
$$\frac{\sigma_E}{E} = \frac{A}{\sqrt{E}} \oplus \frac{B}{E} \oplus X$$

$A/\sqrt{E}$: Statistical fluctuations
B/E: Electronic noise
X: Shower leakage, calibration

Example: ALICE PHOS (Photon Spectrometer)

~18000 $PbWO_4$ crystals





Granularity: 22 x 22 x 180 mm^3
Depth ~ 20 X_0

Electromagnetic sampling calorimeters

Sampling calorimeters: Sensitive layers (e.g. scintillator, semiconductor) sandwiched with passive absorber (high *Z*, e.g. W, Pb).

Resolution of sampling calorimeter:

$$\frac{\sigma_E}{E} = \frac{A}{\sqrt{E}} \oplus \frac{B}{E} \oplus X$$

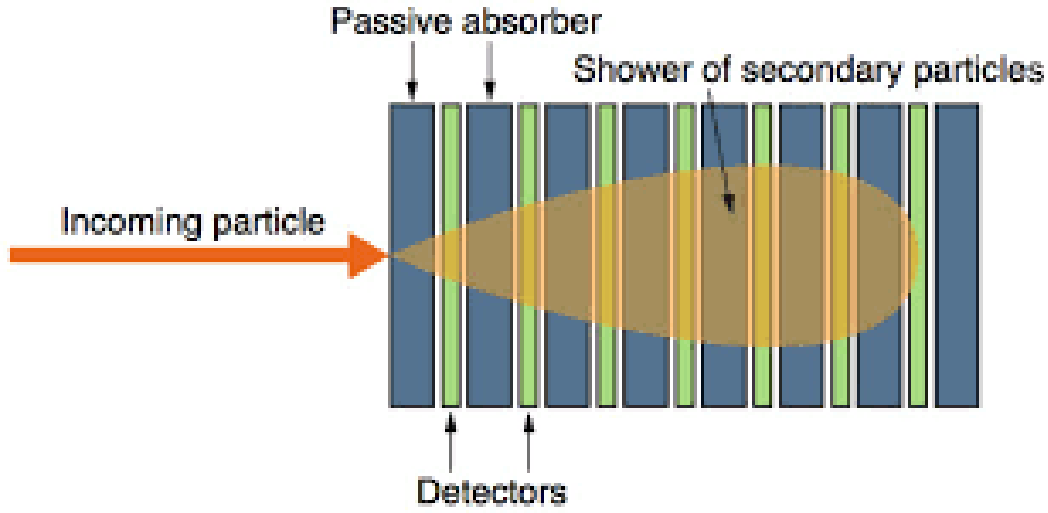
where the term $A/\sqrt{E}$ also contains sampling fluctuations. These depend on the number *n* of track crossings of sensitive layers. Total track length *T* in shower and number of crossings *n*:

$$T \sim N(t_{max}) X_0 = \frac{E}{E_c} X_0; \quad n = \frac{T}{x} = \frac{E}{E_c} \frac{X_0}{x}$$

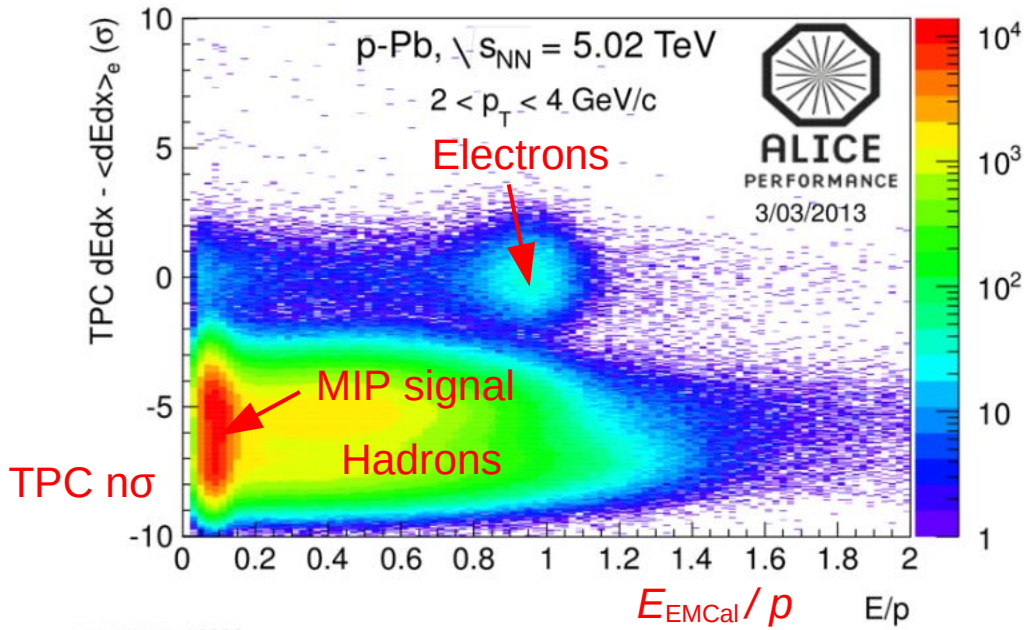
where *N* is number of particles, *x* is sampling layer spacing. Fluctuations assuming independent samplings in each layer – crossings by new set of particles for each layer, Poisson statistics):

$$\frac{\sigma_{\text{samp}}(E)}{E} \sim \frac{1}{\sqrt{n}} = \sqrt{\frac{E_c x}{E X_0}}$$

Thinner layers / more frequent samplings improves resolution.

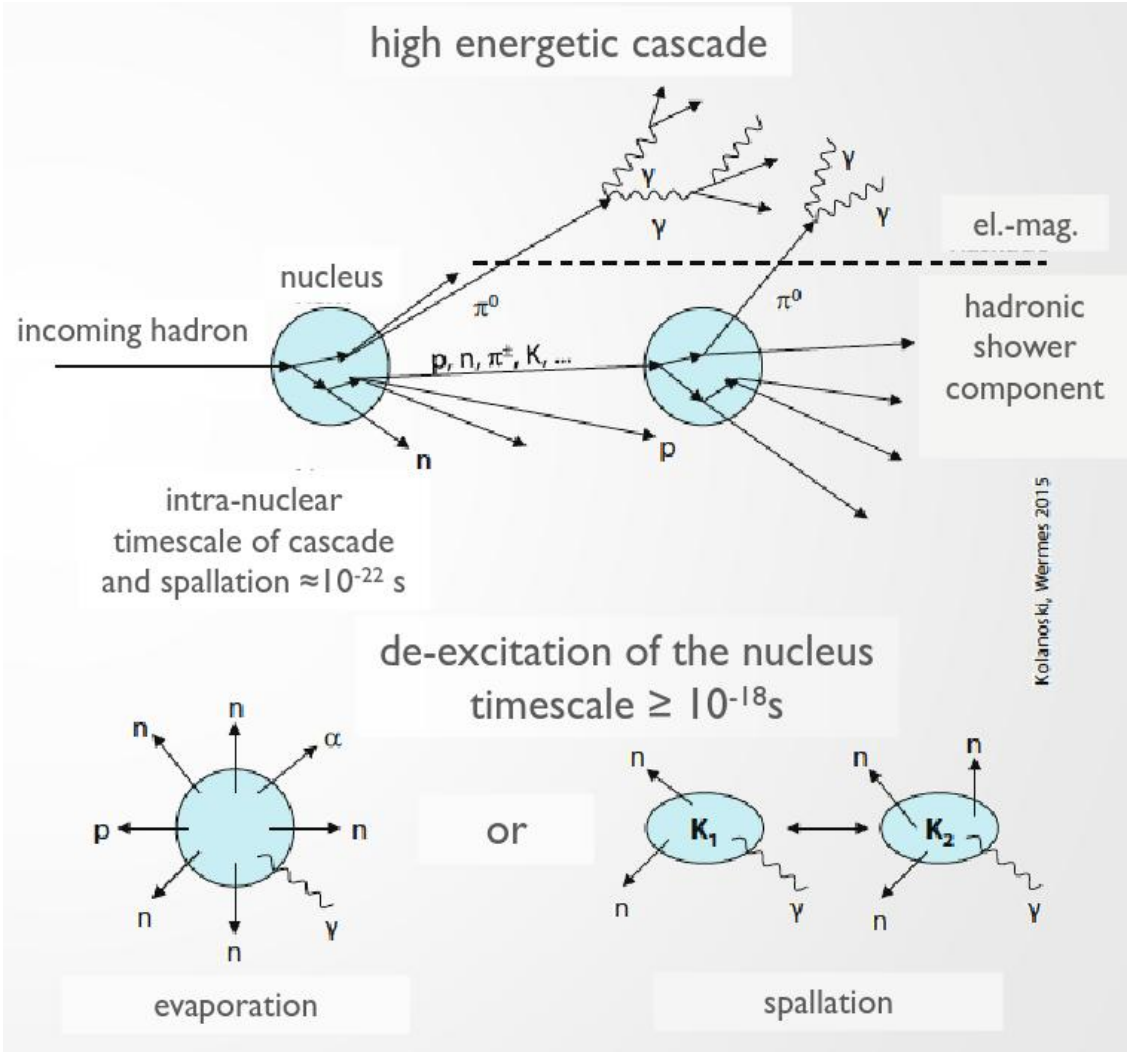


Example: ALICE EMCal (Electromagnetic Calorimeter):
~12000 "towers", 60x60 mm^2 granularity, depth 20.1 X_0. 76/77 alternating layers of Pb absorber, plastic scintillator.

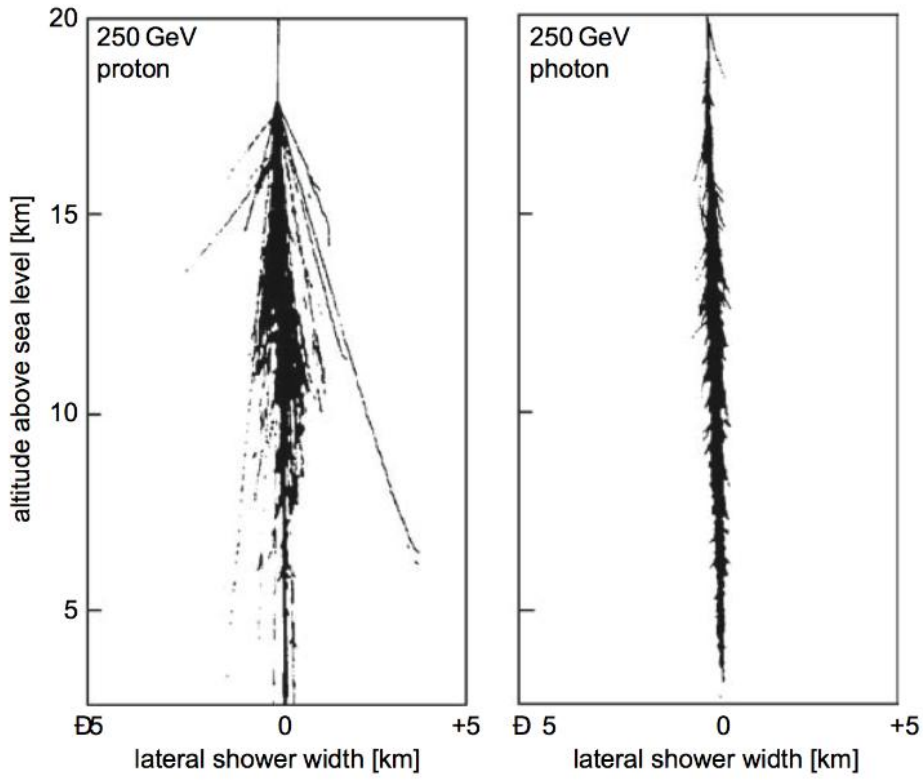


Calorimetry: Hadronic cascades

Hadronic cascade: Successive inelastic interactions of energetic hadrons with nuclei, resulting in multiple production of new hadrons and deexcitation of nuclei involving particle evaporation and nuclear breakup. Charged hadrons and neutrons may initiate new steps in the hadronic cascade. Neutral pions initiate electromagnetic subcascades after diphoton decays (π^0 –> $\gamma\gamma$).
Large invisible energy fraction in hadronic part (nuclear breakup, long-lived neutral particles escaping), large fluctuations in composition –> relatively poor energy resolution.



Spatial development of hadronic showers more chaotic than electromagnetic ones, with larger penetration depths (governed by nuclear interaction length $\lambda_{int} >> X_0$.
Most of the energy deposited early, at a depth near λ_{int} .

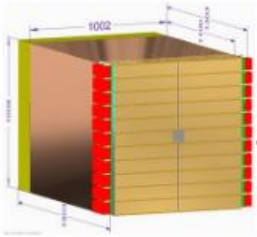


The ALICE detector (Run 3 version)

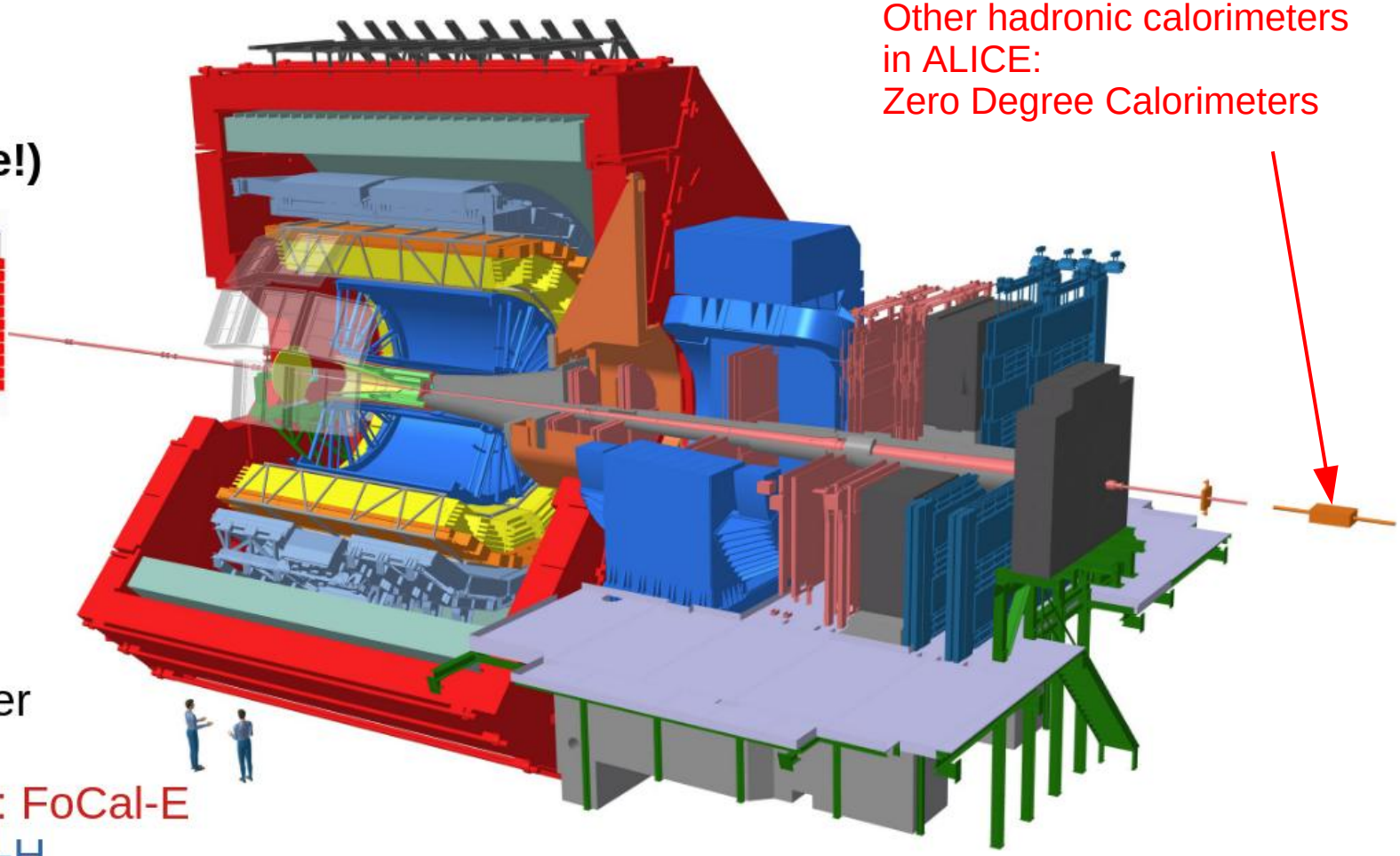
+ FoCal (Forward Calorimeter)

Other hadronic calorimeters in ALICE:
Zero Degree Calorimeters

(not to scale!)



FoCal
$3.2 < \eta < 5.8$

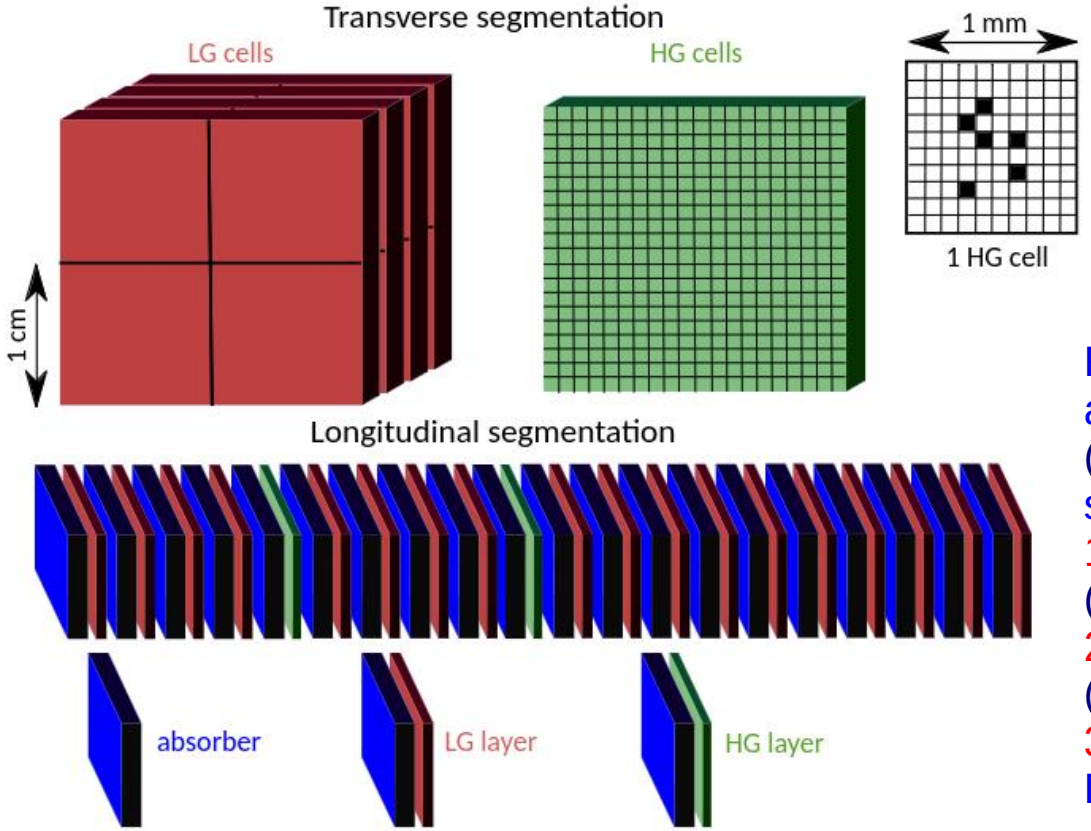


- Forward calorimeter ($3.2<\eta<5.8$)
  - Electromagnetic: FoCal-E
  - Hadronic: FoCal-H

FoCal Technical Design Report

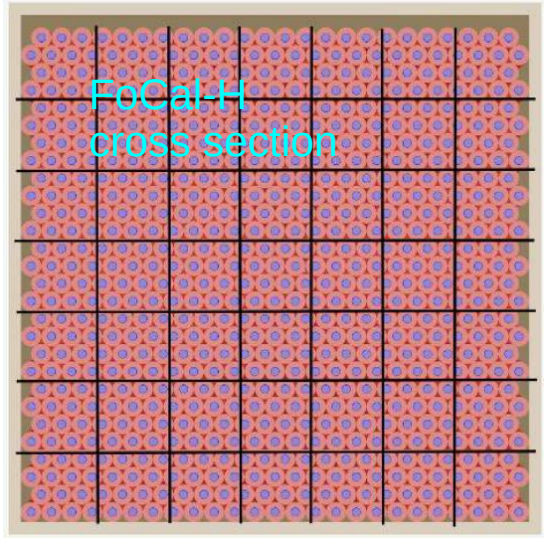
Installation planned before LHC Run 4

ALICE Upgrade: FoCal, an electromagnetic + hadronic calorimeter

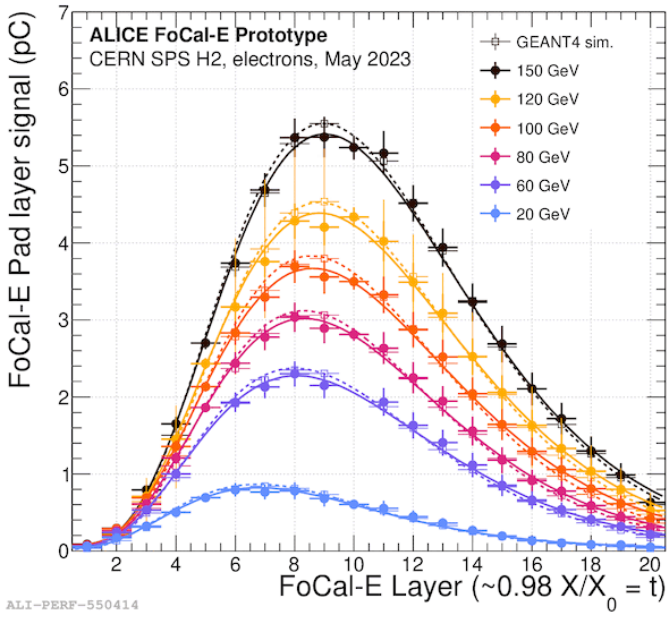


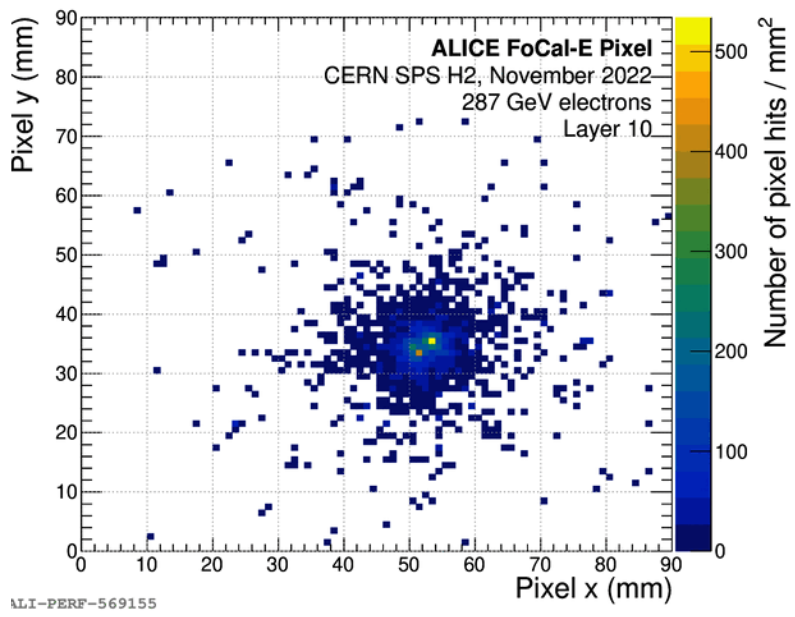
FoCal: Forward spectrometer w/ electromagnetic + hadronic part. Cross section ~ 1 x 1 m^2 .

FoCal-E: 20 W absorber layers (3.5 mm), and Si sensor layers: 18 Si pad layers (1x1 cm^2) and 2 Si pixel layers (ALPIDE MAPS, 30 x 30 μm^2). Depth 17 cm, ~20 X_0 .



Focal-H: Built from Cu capillary tubes (d ~ 2.5 mm) filled with scintillating fibres read out by Si photomultipliers. Depth 110 cm, ~ 5 λ_{int} .

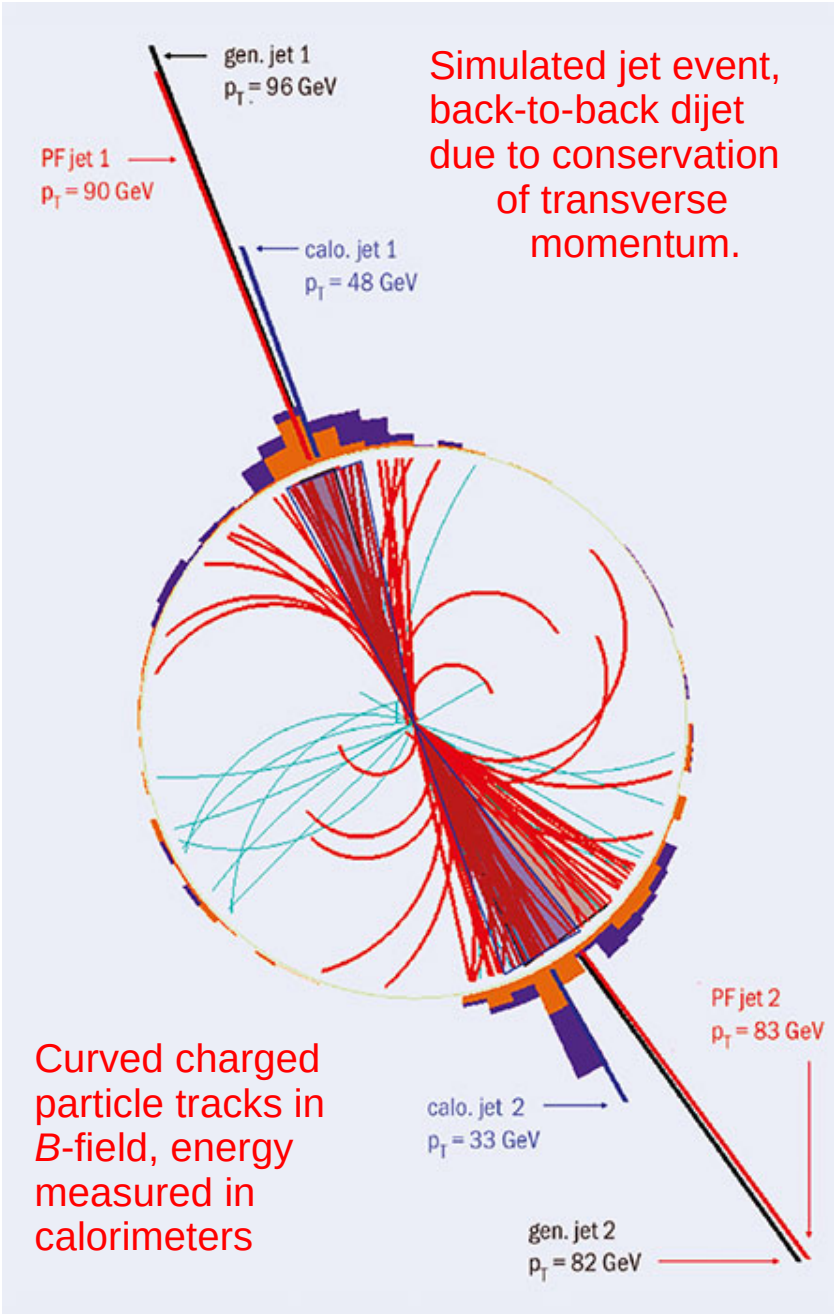




FoCal prototype beam tests at CERN SPS.
Left: Longitudinal profile of electron showers in FoCal-E (data + simulations).
Right: Transverse profile of electron showers in pixel layer (resolved pair of 287 GeV electrons).

Jet measurements

Energetic quarks (and gluons) created in the collision may multiply via various strong processes (quarks may emit gluons, gluons may emit new gluons or split into quark-antiquark pairs). All end up in colourless hadrons (charged / neutral), plus some photons / leptons. This collimated spray of particles is called a jet.



Simulated jet event, back-to-back dijet due to conservation of transverse momentum.

Curved charged particle tracks in *B*-field, energy measured in calorimeters

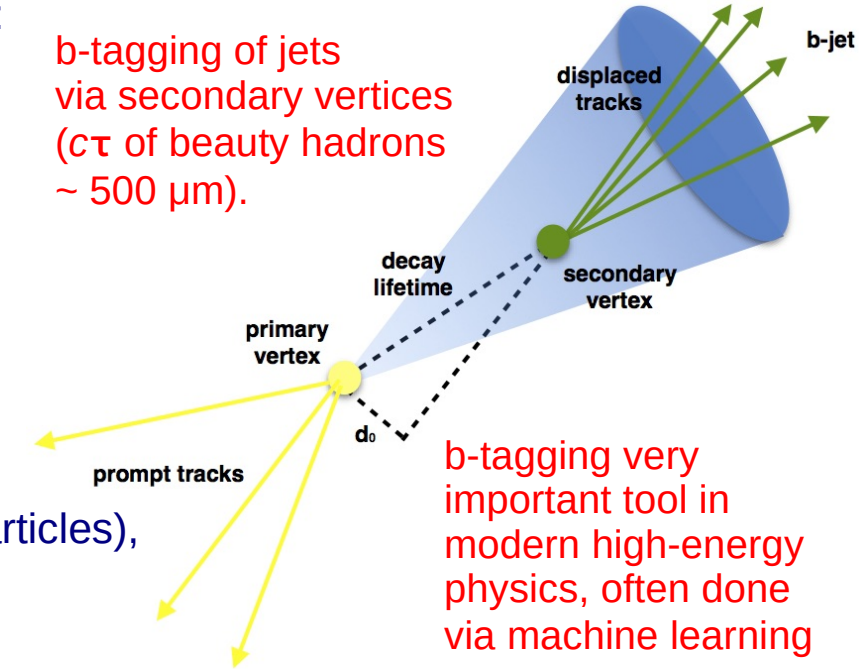
ALICE measures charged (parts of) jets using the central barrel tracking system, and also full jets including neutral energy, combining tracking with clusters in the EM calorimeter (largest contribution neutral pions, π^0 –> γγ).

Challenge: Jet energy scale. OK for charged part of jet since tracking provides momenta *p*. EMCal cluster energy must be corrected for charged particle contamination, using track extrapolation and assuming MIPs. Some energy remains invisible (e.g. neutrons, neutrinos).

ALICE jet measurements mostly focus on charged jets and their substructure at relatively low p_T .

Very interesting: Substructure of b- and c-jets vs light quark / gluon jets.

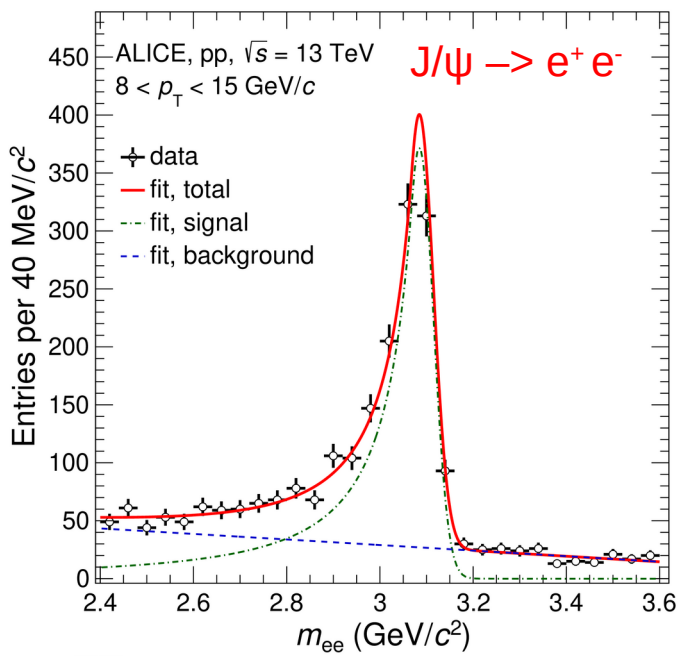
b-tagging of jets via secondary vertices ($c\tau$ of beauty hadrons ~ 500 μm).



Particle physics: b-jets important decay products of Higgs bosons (and possible undiscovered particles), crucial to catch full energy.

b-tagging very important tool in modern high-energy physics, often done via machine learning

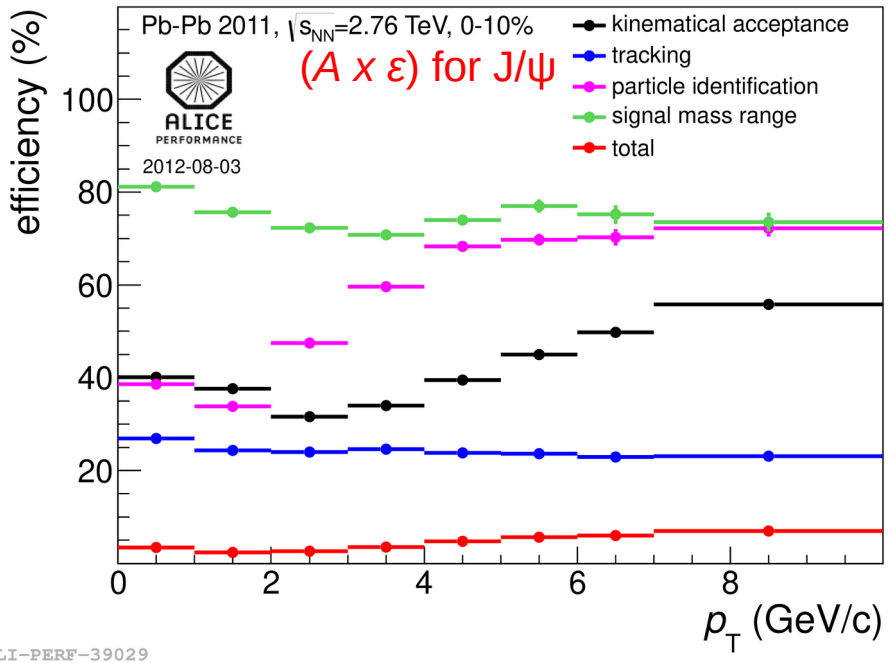
Extraction of production cross sections (1)



Measurements are typically quantified as differential cross sections (σ) in a specific kinematic window, e.g. (y, p_T):

$$\frac{\mathrm{d}^2\sigma}{\mathrm{d}y\mathrm{d}p_\mathrm{T}} = \frac{N_{\mathrm{raw,J}/\psi}(\Delta y, \Delta p_\mathrm{T})}{\mathrm{BR}(\mathrm{J}/\psi \to e^+e^-) \cdot (A \times \epsilon)(\Delta y, \Delta p_\mathrm{T}) \cdot \Delta y \cdot \Delta p_\mathrm{T} \cdot L_\mathrm{int}}$$

N_{raw}: Raw yield of the particle species measured in the kinematic window of interest, (Δy, Δp_T).
BR(X –> Y_1 Y_2), branching ratio: Fraction of the mothers X decaying into the set of daughters Y used for reconstruction.
(A x ε), acceptance times efficiency correction, is related to the detector setup and the data analysis.



Acceptance A: Probability for the particles to reach the detector geometrically and deposit a potentially detectable signal (may include kinematic cuts).
Efficiency ε: Product of several factors related to detector and analysis, typically including:

Tracking efficiency: Probability for reconstructing the track / decay topology of the particle
PID efficiency: Probability of correctly identifying the particle species of relevant tracks
Signal mass range: Fraction within integrated range of signal peak in invariant mass spectrum

Extraction of production cross sections (2)

Differential production cross section: Important, normalised quantity for comparison with theory and between experiments.

$$\frac{\mathrm{d}^2\sigma}{\mathrm{d}y\mathrm{d}p_\mathrm{T}} = \frac{N_{\mathrm{raw,J}/\psi}(\Delta y, \Delta p_\mathrm{T})}{\mathrm{BR}(\mathrm{J}/\psi \to e^+e^-) \cdot (A \times \epsilon)(\Delta y, \Delta p_\mathrm{T}) \cdot \Delta y \cdot \Delta p_\mathrm{T} \cdot L_\mathrm{int}}$$

(A x ε) is calculated via Monte Carlo simulations which incorporate the detailed detector setup (geometry and materials) with time dependent detector conditions, generated particles with realistic kinematic distributions, and application of the same reconstruction and analysis algorithms to simulated as to experimental data.

$(A \times \varepsilon) = N_{\mathrm{reconstructed}} / N_{\mathrm{generated}}$

where $N_{\mathrm{generated}}$ is the number of particles generated in the simulation, $N_{\mathrm{reconstructed}}$ is the number of simulated particles correctly reconstructed.

More on simulations by Kyrre Sjøbæk (GEANT4).

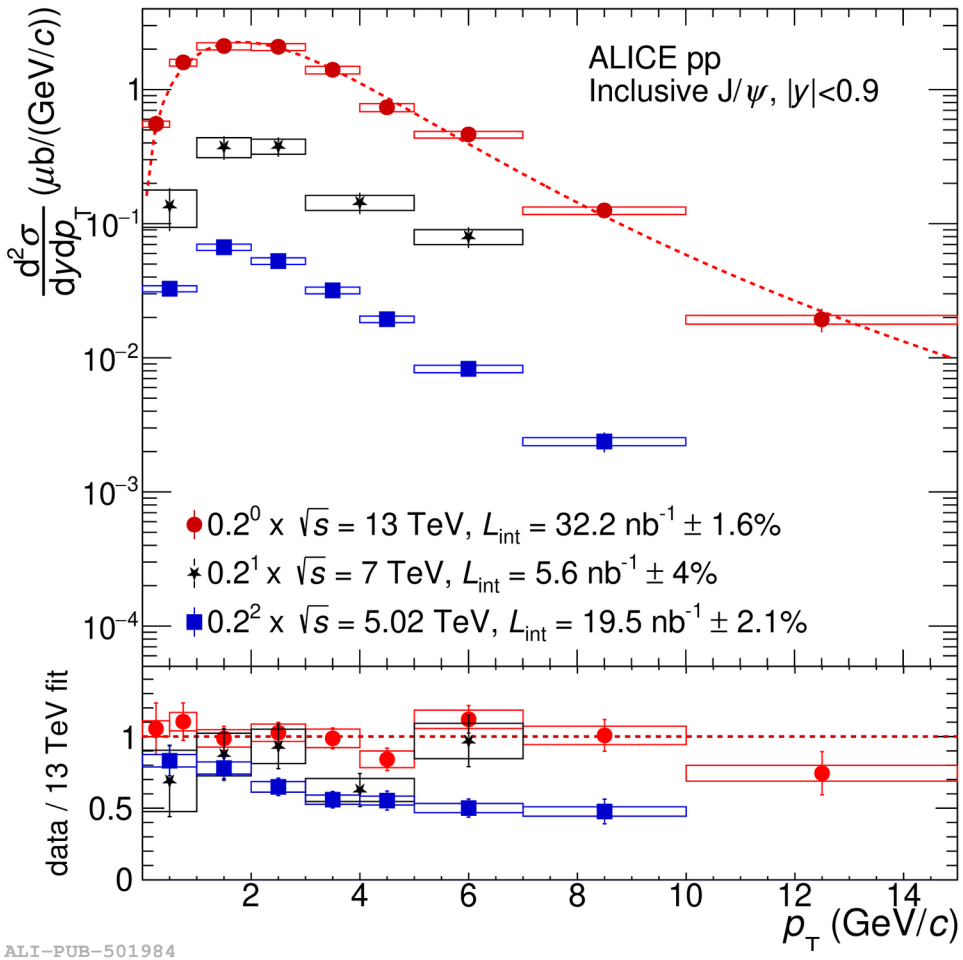
Luminosity very important for normalisation:

L_{int}: Integrated luminosity, $L_{int} = \int L_{inst}\, dt$ (area)$^{-1}$

L_{inst}: Instantaneous luminosity – depends on properties of colliding beams, ~ (area)$^{-1}$ (time)$^{-1}$

(Reminder: $L_\mathrm{inst} = \frac{N_1 N_2 f N_\mathrm{bunch}}{4\pi\sigma_x\sigma_y}$)

Differential cross section for J/ψ in pp@13 TeV



Extraction of other observables (nuclear modification / flow)

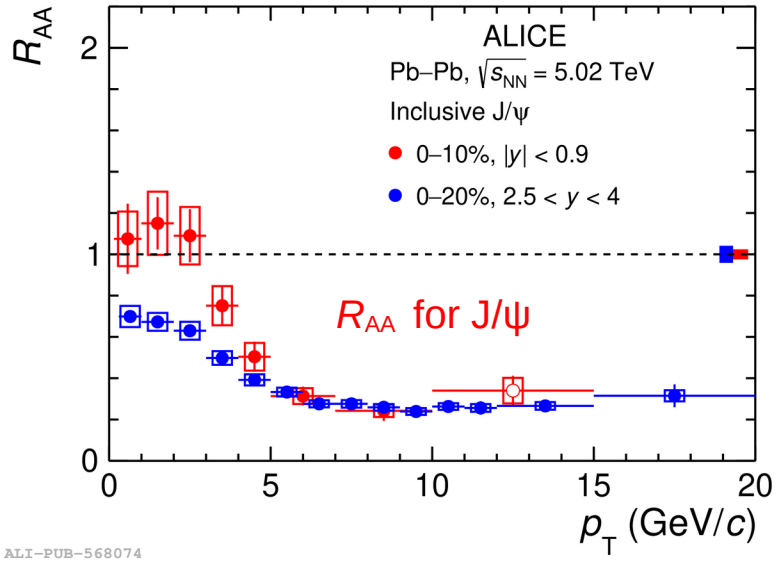
Important observables in heavy-ion physics, using other normalisation approaches:

Nuclear modification factor R_{AA} (AA yields normalised to pp yields):

$$R_{\mathrm{AA}} = \frac{\mathrm{d}^2 Y_{\mathrm{AA}}/\mathrm{d}y\mathrm{d}p_{\mathrm{T}}}{\langle N_{\mathrm{coll}}\rangle \mathrm{d}^2 Y_{\mathrm{pp}}/\mathrm{d}y\mathrm{d}p_{\mathrm{T}}}$$

$Y_{AA,\ pp}$ – yield per event

$\langle N_{coll} \rangle$: number of nucleon-nucleon collisions per AA interaction



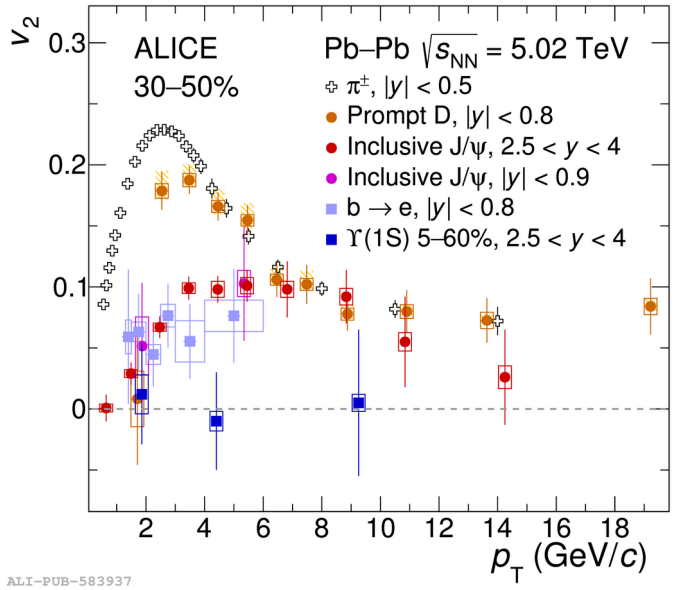
R_{AA}: Quantify quark energy loss in QGP and other medium effects – suppression from dissociation of hadrons (R_{AA} < 1), enhancement from recombination of quarks into hadrons (R_{AA} > 1).

Collective anisotropic flow v_n:

$$\frac{\mathrm{d}N}{\mathrm{d}\phi} \propto 1 + \Sigma_{\mathrm{n}} v_{\mathrm{n}} \cos\left[\mathrm{n}(\phi - \Psi_{\mathrm{n}})\right]$$

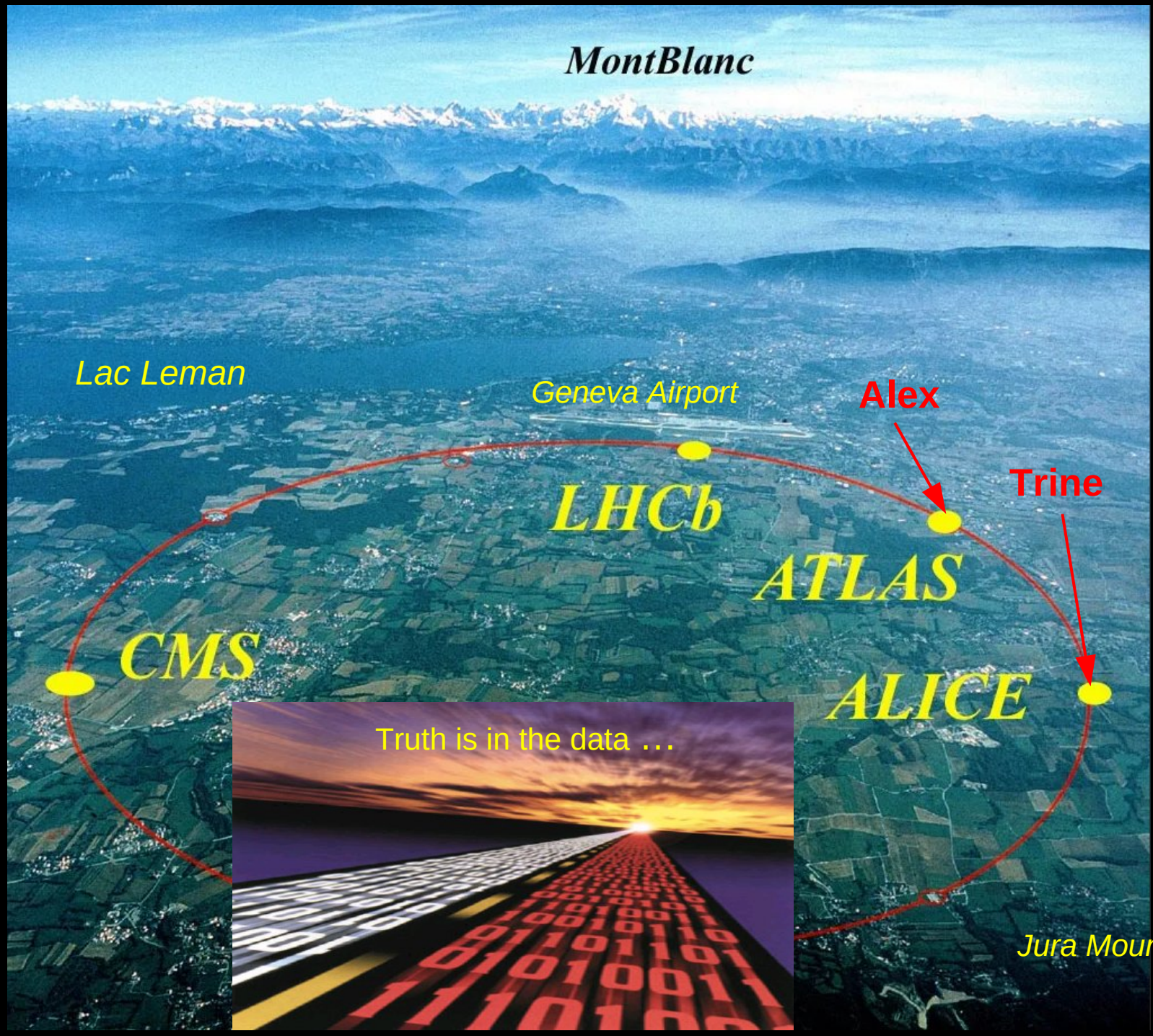
Fourier decomposition of azimuthal distribution harmonic coefficients v_n (ψ_n is event symmetry plane)

v_2 (elliptic flow) for different hadron species



v_n: Quantify collective anisotropic flow – hydrodynamic behaviour, extent of quark thermalisation in medium.

LHC experiments – charting unknown and exotic territory!



Possible questions for the FYS4505 examination

– How can we verify that a heavy-ion collision (event) has taken place, and how can we determine the collision centrality?

– Describe the layout of a generic high-energy physics detector and the functionality of the different layers. How can we detect e.g. muons, photons, protons, neutrons, electrons and neutrinos?

– How are charged particle tracks and primary / secondary vertices registered? What factors determine the vertex resolution and the track momentum resolution?

– Describe some techniques for identification of charged particles.

– How can very short-lived particles be detected and identified?

– Describe briefly the development of electromagnetic and hadronic cascades. How can they be detected in electromagnetic and hadronic calorimeters?